New opportunities in metallurgy: High Entropy Alloys – fabrication methods, microstructure, properties

Tomasz Stasiak

Masaryk University, Brno, Czech Republic

Warsaw, the 31st of January 2022

Outline

1. Introduction of high entropy alloys
- Definition
- Common compositions
- Common properties

2. Fabrication methods
- Liquid state
- Solid state
- Plasma deposition

3. Conclusions and future prospects

1.1. Introduction – High Entropy Alloys – History and Definitions

- New group of multi-elemental metallic materials (2004 *);
- Infinite possibilities of new chemical compositions;
- No consensus on definition ➔ two definitions.

The first definition of high entropy alloys (HEAs)

Alloys: at least five main elements, each with content between 5 and 35 at. %.

$$n_{main} > 5 \text{ and } 5 \text{ at. } \% < c_i < 35 \text{ at. } \%$$

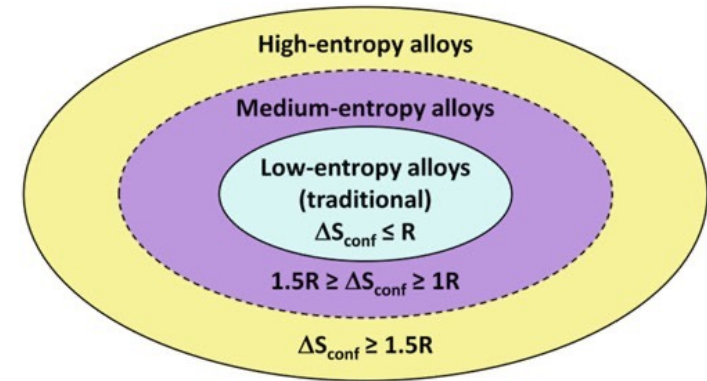The second definition of high entropy alloys (HEAs)

Alloys with configuration entropies greater than 1.5R (R is the gas constant).

$$\Delta S_{conf} > 1.5 \text{ R}$$

High mixing entropy (especially configurational entropy) ➔
Formation of solid solutions.

$$\Delta G_{mix} = \Delta H_{mix} - T\Delta S_{mix}$$

* B. Cantor et al., Mater. Sci. Eng. A. 375–377 (2004) 213–218.
J.-W. Yeh et al., Adv. Eng. Mater. 6 (2004) 299–303.
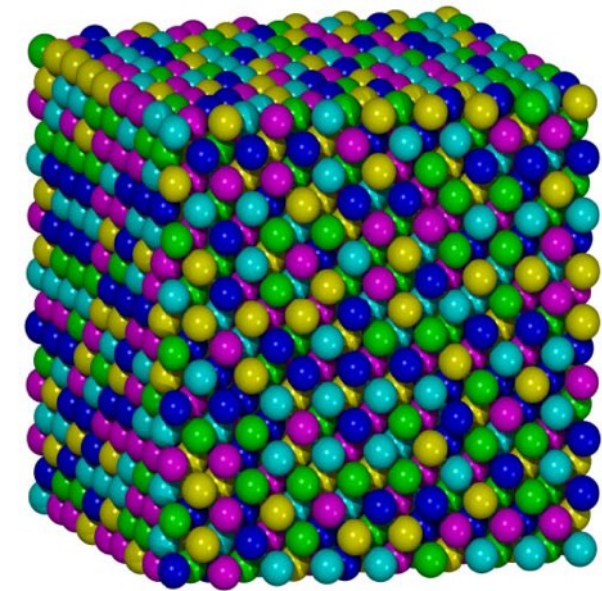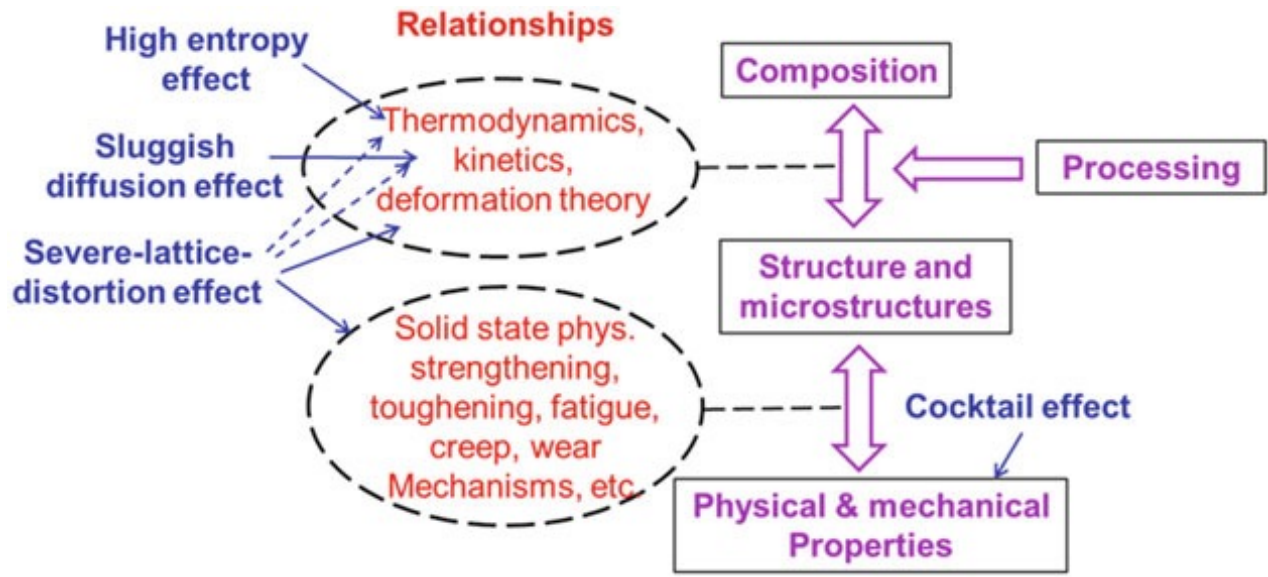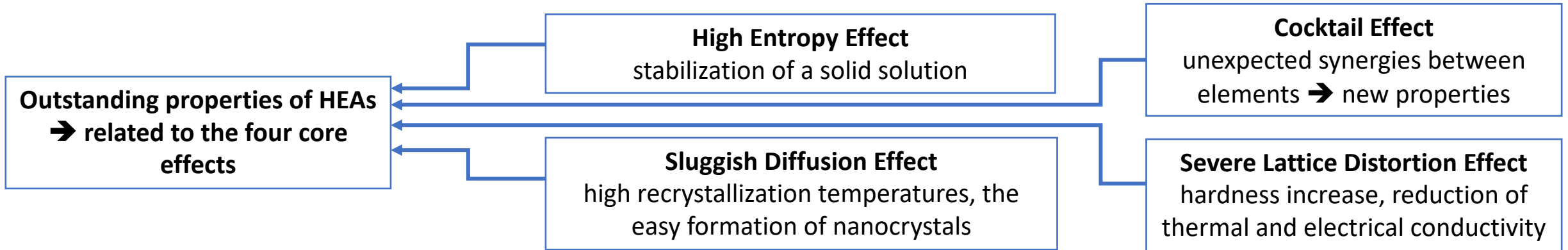
Types of alloys based on configurational entropy.

M.C. Gao, P.K. Liaw, J.W. Yeh, Y. Zhang, High-entropy alloys:
Fundamentals and applications, Springer International Publishing, 2016.
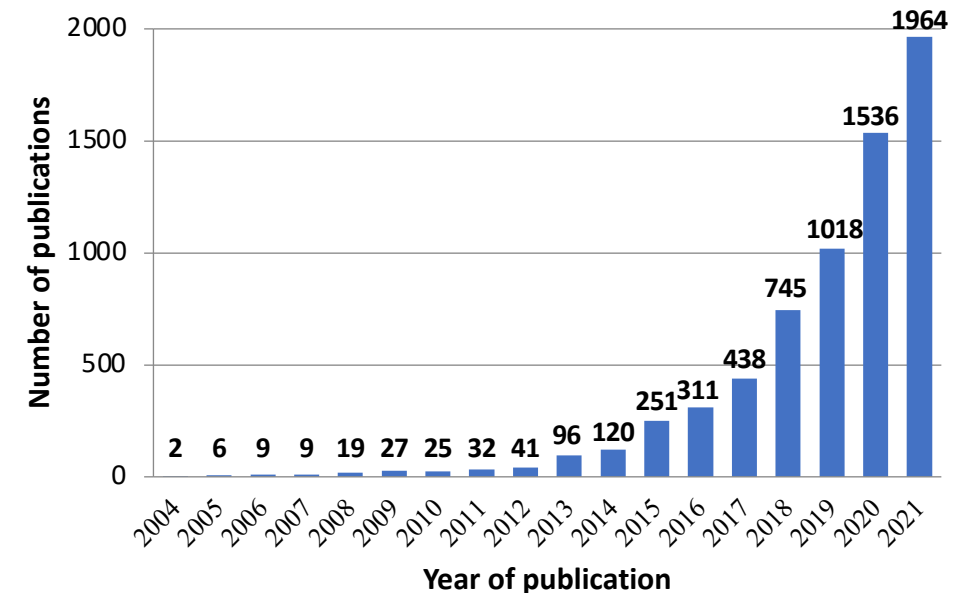
Number of publications on HEAs based on Scopus analysis.

1.2. Introduction – High Entropy Alloys – History and Definitions

High Entropy Effect
stabilization of a solid solution

Cocktail Effect
unexpected synergies between elements ➔ new properties

Outstanding properties of HEAs ➔ related to the four core effects

Sluggish Diffusion Effect
high recrystallization temperatures, the easy formation of nanocrystals

Severe Lattice Distortion Effect
hardness increase, reduction of thermal and electrical conductivity


The scheme of physical metallurgy in which those areas influenced by the four core effects of HEAs are indicated.

*Atomic structure model of fcc CoCrFeMnNi.*

1.3. Introduction – High Entropy Alloys – common compositions

- Many HEAs present simple structure:
  - face-centered cubic (fcc);
  - body-centered cubic (bcc);
  - hcp hexagonal close-packed (hcp).
- Multiphase HEAs, sometimes named compositionally complex alloys (CCAs) – a mixture of bcc, fcc, hcp, ordered phases – e.g., high entropy superalloys.
- Most commonly studied – the CoCrFeMnNi system (Cantor family) revealing fcc single solid solution.
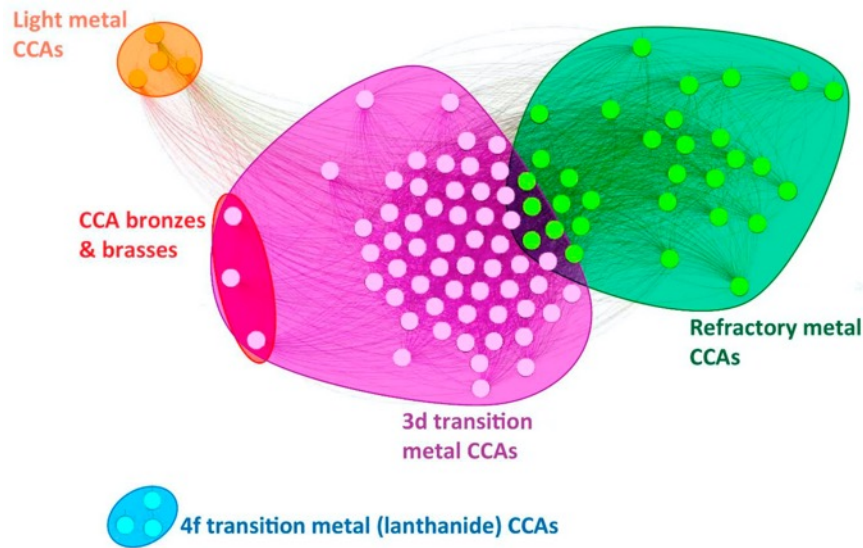
Alloy network of 110 equiatomic HEAs/CCAs showing five main categories. Dots represent alloys, lines represent sharing one or more elements.
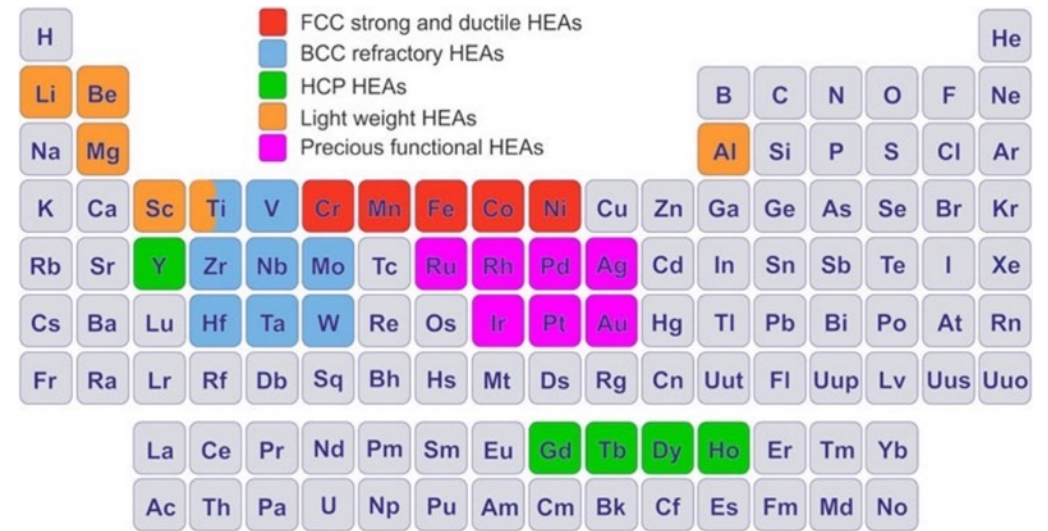
Most often used elements to form HEAs.

1.4. Introduction – High Entropy Alloys – common properties

Exceptional properties of many HEAs:

- Cantor alloy (CoCrFeMnNi): high tensile strength, ductility, and toughness at low (cryogenic) temperatures.
- Refractory alloy (NbMoTaW): promising mechanical properties at high temperatures under compression.

Other properties often discussed in the literature:
- Good wear, creep resistance, and thermal stability.
- Resistance to oxidation, hydrogen embrittlement, and corrosion.
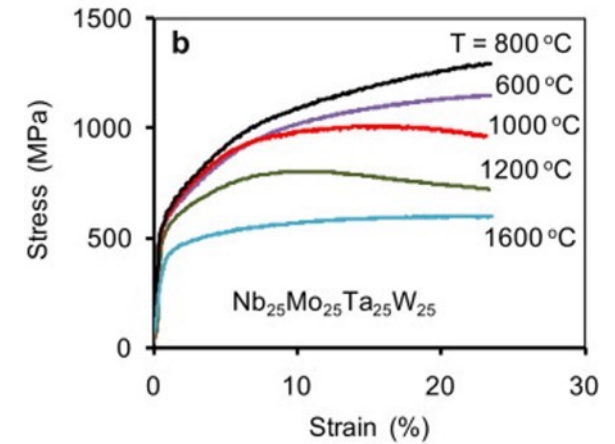- Irradiation resistance.
- Good weldability.

Compression results for the NbMoTaW.

O.N. Senkov et al., Intermetallics 19 (2011) 698-706
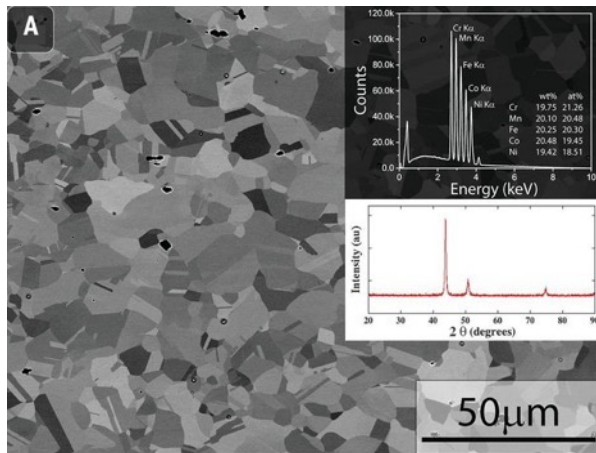
Fully recrystallized microstructure of single fcc phase CoCrFeMnNi alloy.
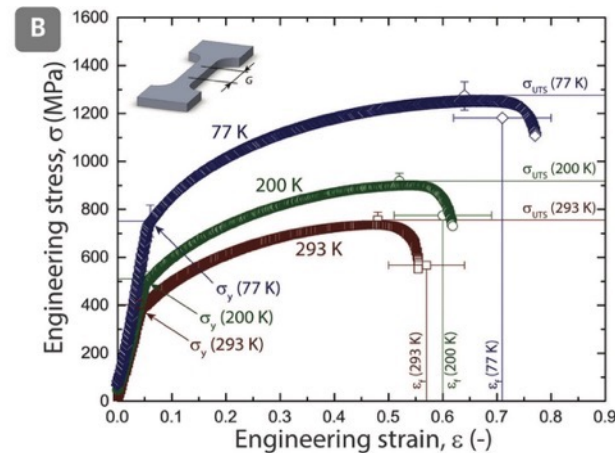
Tensile results of CoCrFeMnNi alloy tested at different temperatures (77 K, 200 K, 293 K).
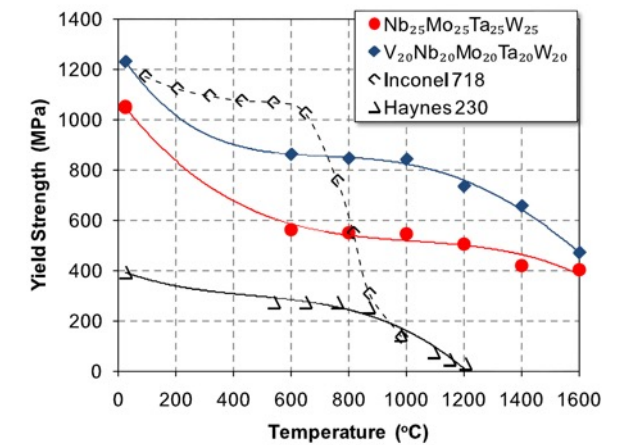
Temperature dependence of the yield stress of two HEAs and two superalloys.

2. Fabrication methods (FM) – overview
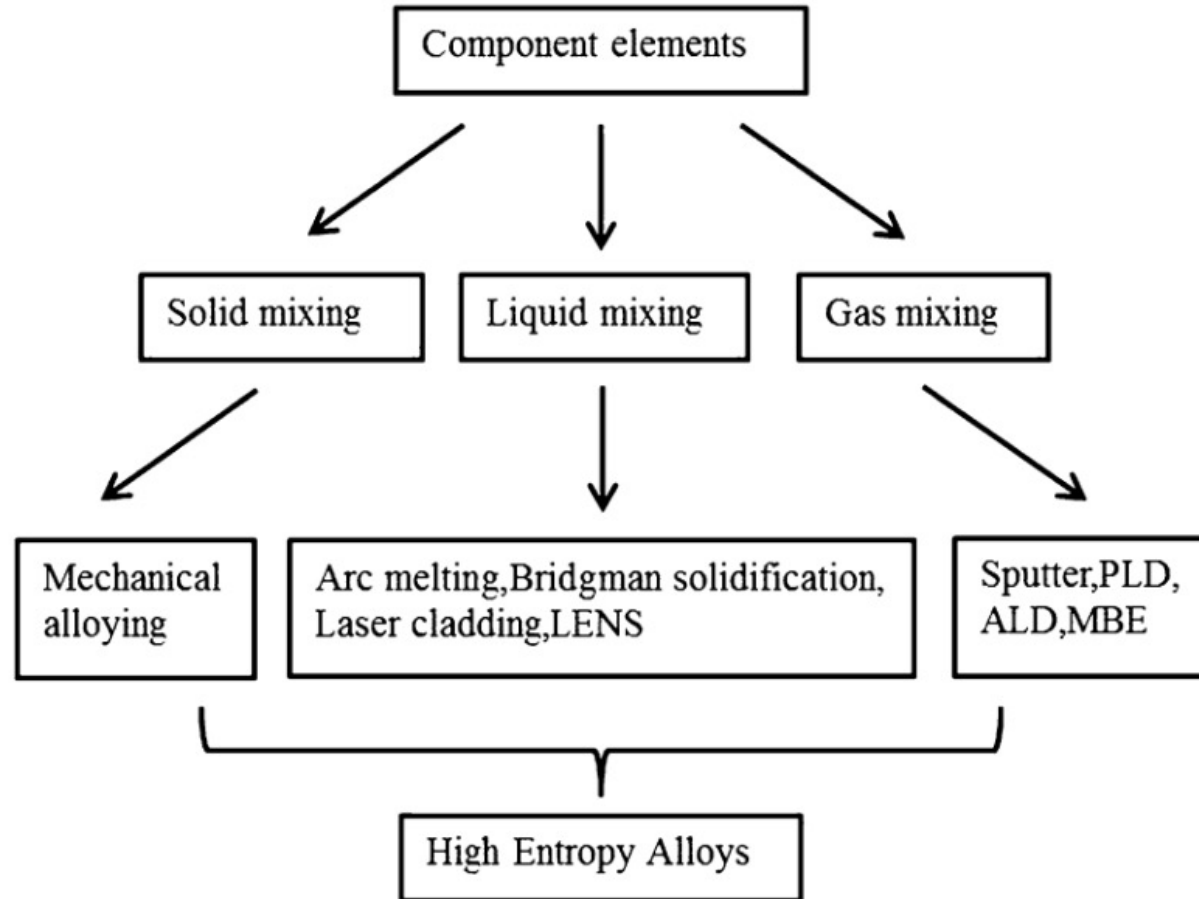
Summary of fabrication routes for HEAs.

M.C. Gao, P.K. Liaw, J.W. Yeh, Y. Zhang, High-entropy alloys: Fundamentals and applications, Springer International Publishing, 2016.

2.1.1. FM – liquid state

- Preparation in the liquid state ➔ the most common for HEAs as for other metallic materials.

- Casting = many advantages (easy and relatively low-cost fabrication of HEAs), however some problems, e.g., dendritic segregation (annealings needed).

- Additive manufacturing ➔ very rapid development of these techniques (high precision of the parts with a complex shape, minimal material loss, different parameters to control microstructure and properties).
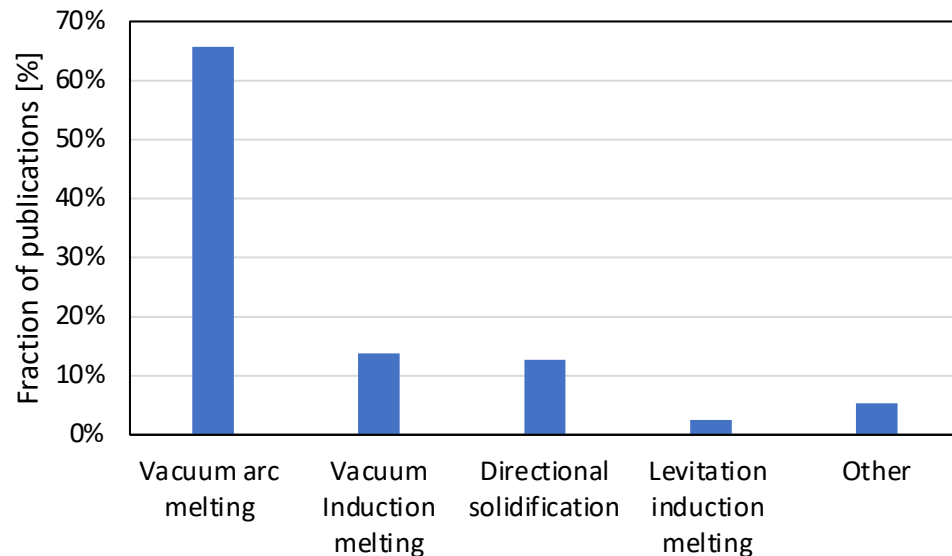
*Distribution of works published depending on casting technologies used for HEAs production.*
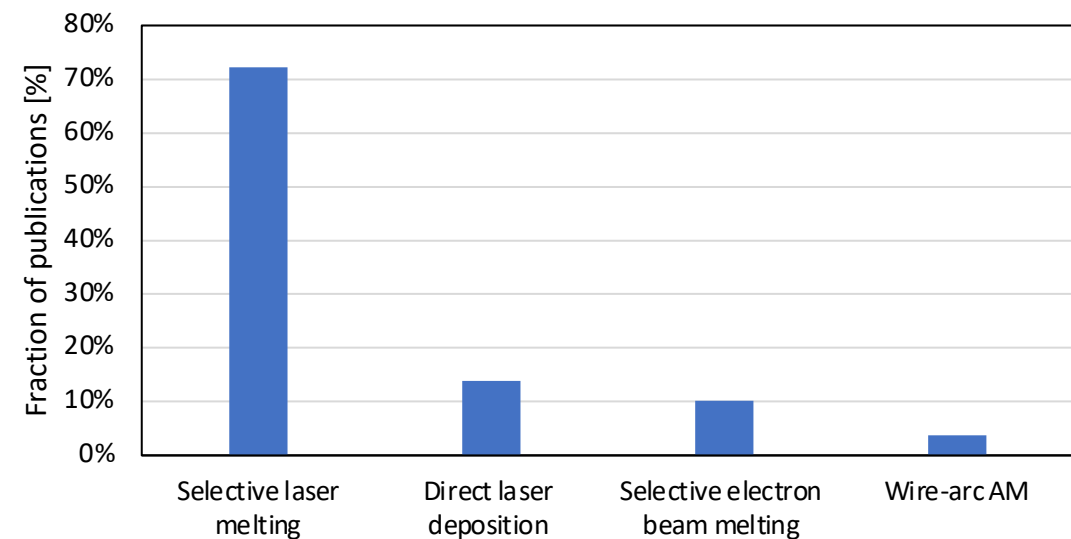
Distribution of works published depending on technologies of additive manufacturing used to produce HEAs.

V. E. Gromov, S. V. Konovalov, Yu. F. Ivanov, K. A. Osintsev, Structure and Properties of High-Entropy Alloys, Springer 2021

V. E. Gromov, S. V. Konovalov, Yu. F. Ivanov, K. A. Osintsev, Structure and Properties of High-Entropy Alloys, Springer 2021

2.1.2. FM – liquid state – CoCrFeMnNi melt spinning

Effects of solidification conditions on microstructure and properties of high entropy alloys from the CoCrFeMnNi family.

- Cold crucible cast high entropy alloys were melted and then cast by melt spinning.

- Very fast cooling rates: in order of 10^5-10^6 K s^{-1} depending on the wheel rotation speed.

- Addition of niobium and carbon to increase hardness.

- Structure/microstructure studied by XRD, SEM-EDX, EBSD, TEM-EDX.
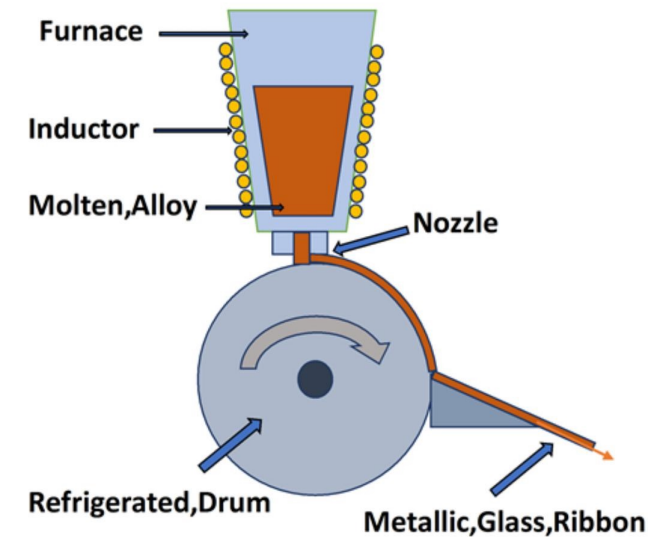
Scheme showing melt spinning process.

X. Liang, J. Chen, M.T. Mora, J.F. Urdaneta, Q. Zeng, Advances in Materials Physics and Chemistry, Vol.7 No.6, 2017.
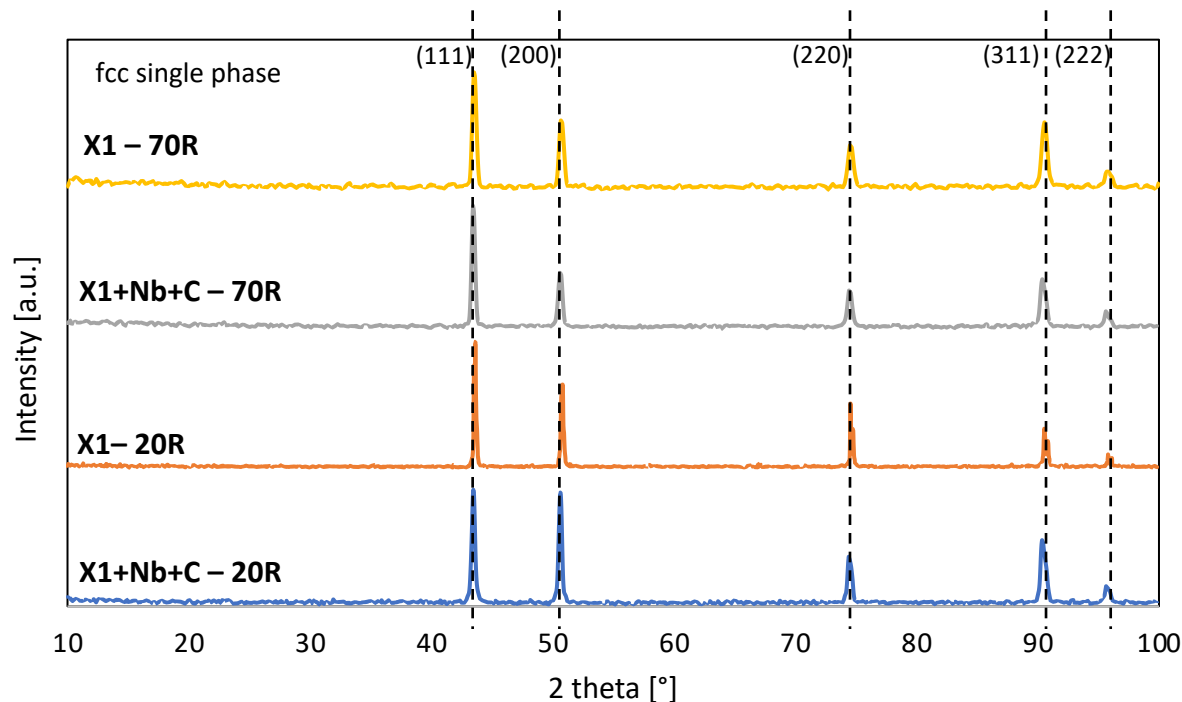
Sample	Composition	Wheel rotation (cooling rate)
X1	Equiatomic CoCrFeMnNi	20R and 70R
X1+Nb+C	CoCrFeMnNi + 1.30 wt.% Nb + 0.02 wt.% C	
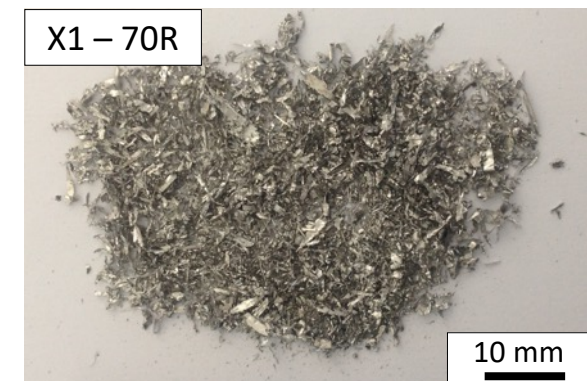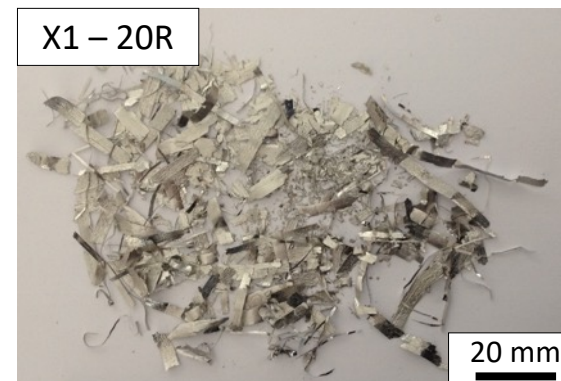
Ribbons obtained by melt-spinning.

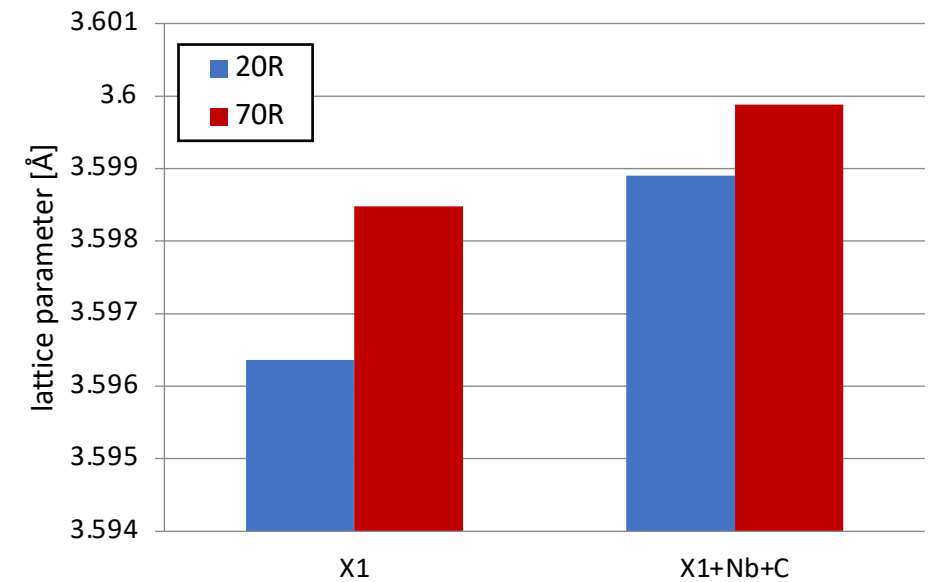# 2.1.3. FM – liquid state – CoCrFeMnNi melt spinning

- Fcc single-phase present in all studied samples.

- No peaks of other phases, e.g., NbC (low volume fraction?).

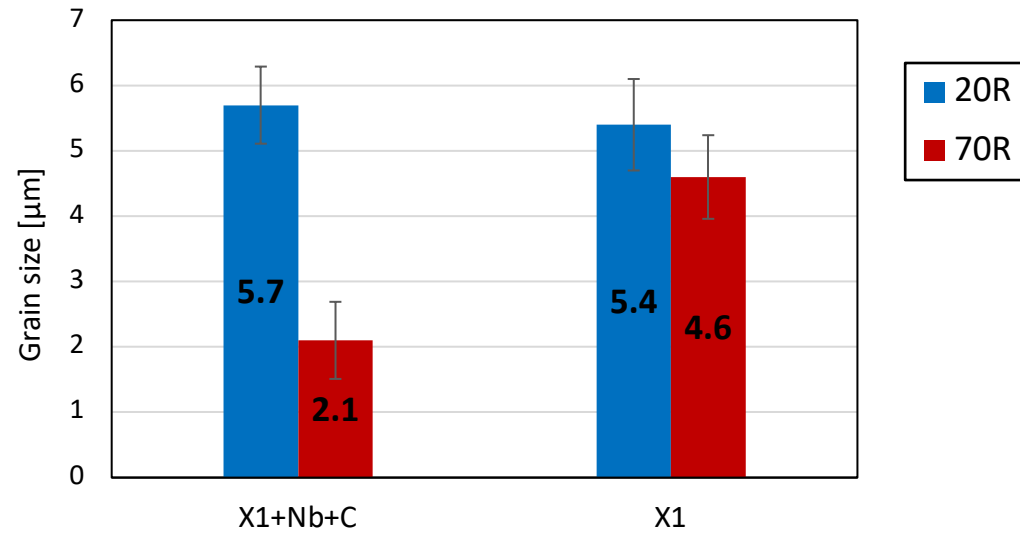- All samples well crystalized ➔ no amorphous structure.

Lattice parameter:
- A higher solidification rate increases the lattice parameter.
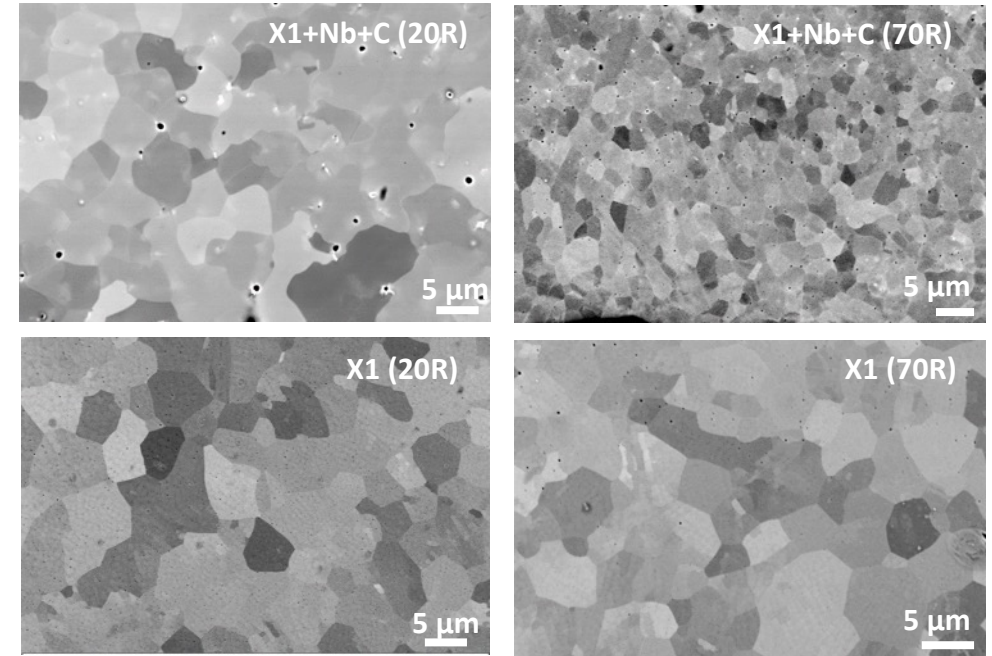- The presence of Nb and C also increases the lattice parameter.

XRD patterns of melt-spun ribbons.

Lattice parameter of fcc phase of melt-spun ribbons.

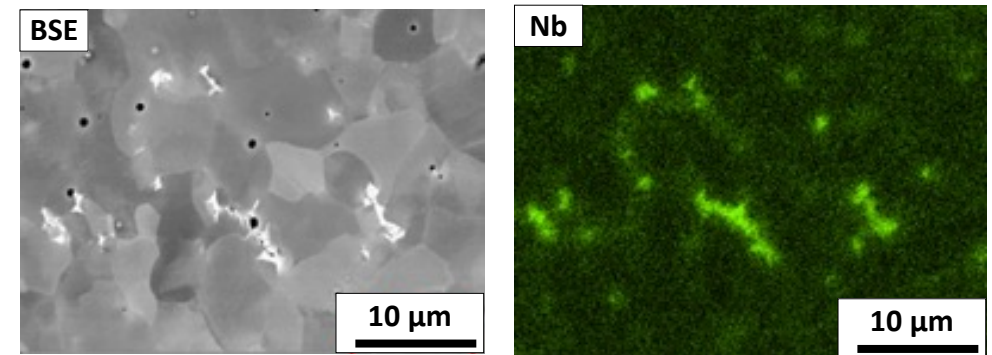# 2.1.4. FM – liquid state – CoCrFeMnNi melt spinning

- Microstructure consists of equiaxed, fine grains (a few micrometers).

- Grain size decreases with faster cooling rate.

- In the samples with addition of Nb and C ➔ visible zones located at grain boundaries enriched in niobium and carbon.

SEM-BSE images of microstructure of produced ribbons.

Average grain size of produced ribbons.

SEM-BSE image and EDX map showing Nb-rich zone in the produced ribbon.
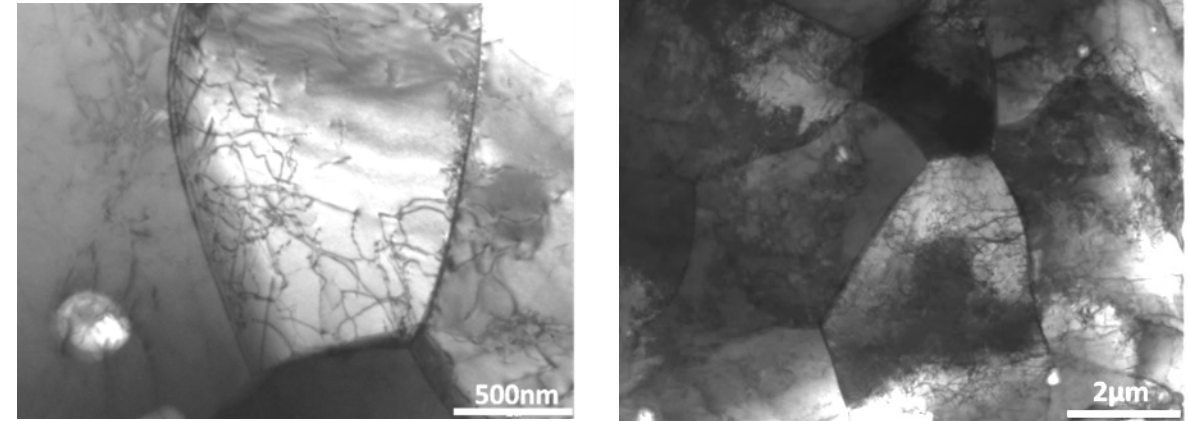
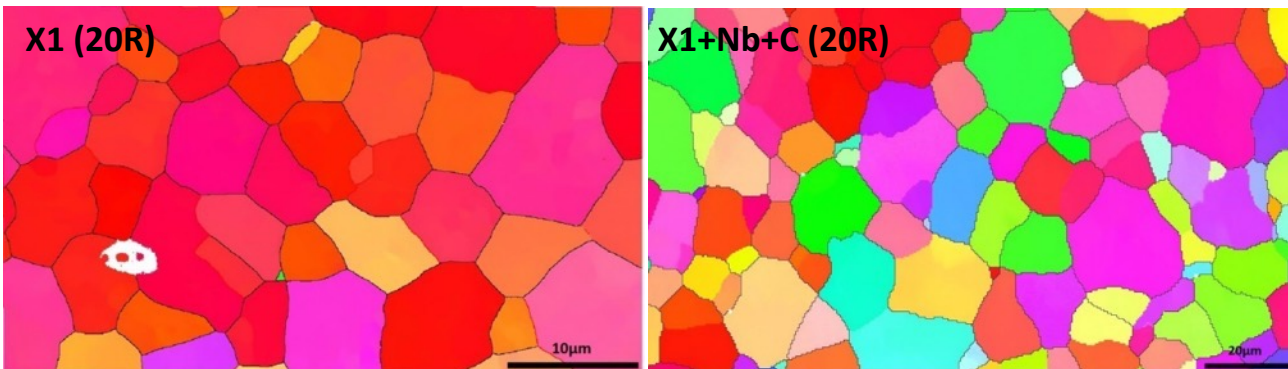# 2.1.5. FM – liquid state – CoCrFeMnNi melt spinning

EBSD results

- Orientation inside grains is almost homogeneous.

- Twin boundaries have not been detected in any samples.
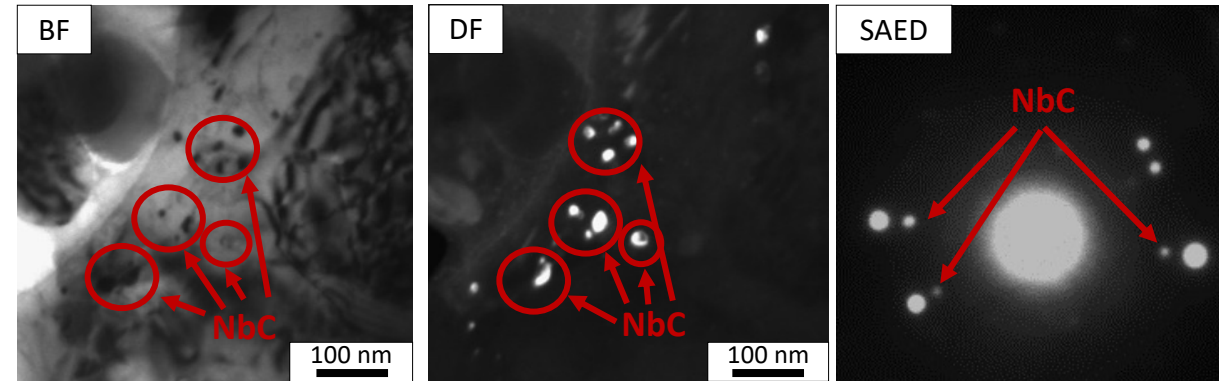
TEM results

- High density of dislocations is present in all studied samples.

- NbC nanometric size precipitates are present in alloys with the addition of Nb and C.

TEM-BF images of grains of X1 (20R) sample.


EBSD inverse pole figure images of produced ribbons.

TEM analyses of X1+Nb+C (70R).

2.1.6. FM – liquid state – CoCrFeMnNi melt spinning

- Higher cooling rate ➔ slightly higher hardness.
- Slightly higher hardness of alloy containing Nb and C than pure alloy.

- Increase of hardness of samples containing C and Nb after annealing at 500°C for 24h ➔ formation of a higher volume fraction of NbC carbide (nanoprecipitates).
- Decrease of hardness of samples without Nb and C ➔ grain growth.

Conclusions

- CoCrFeMnNi alloy presents an fcc crystal structure after all studied cooling conditions. No amorphous phase was observed.
- Microstructure of all alloys consists of fine equiaxed grains of a few micrometers size.
- High density of dislocation has been found in all alloys. Twin boundaries have not been detected. Orientation inside grains is homogenous.
- Hardening due to nanoprecipitates (NbC) was obtained through 500°C/24h annealing.

Hardness of melt-spun ribbons.

Hardness of melt-spun ribbons before and after annealing.
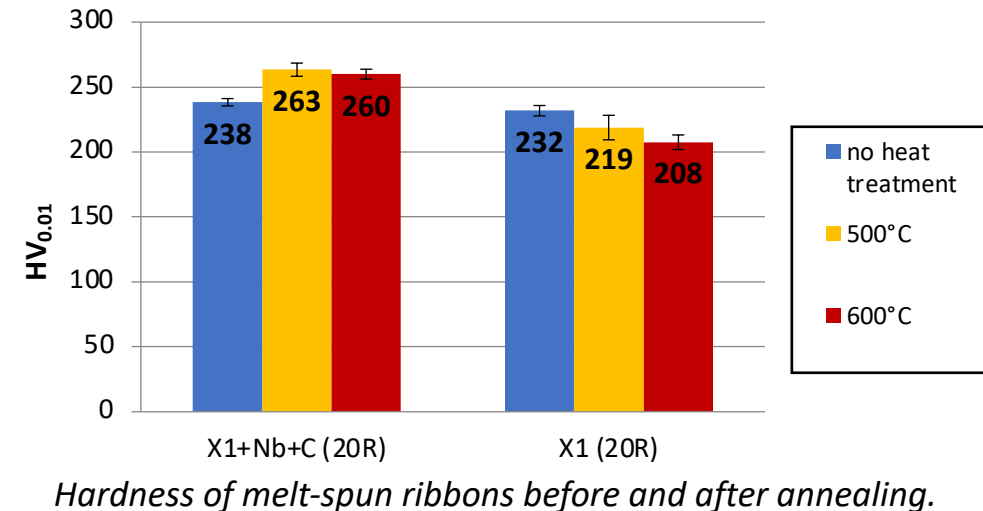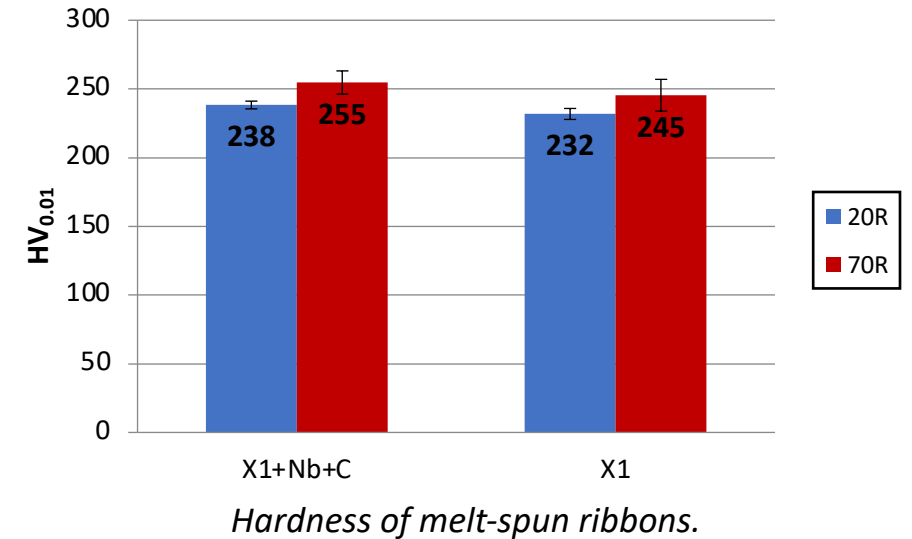
# 2.2.1. FM – solid state – mechanical alloying

Rapid development of HEAs produced by powder metallurgy, mainly by mechanical alloying and sintering.

Advantages of mechanical alloying + sintering:
- Easy to obtain a fine microstructure without segregation problems;
- No solubility problems of metals in the liquid phase (no melting);
- Possibility of preparing alloys with large differences in melting temperature between elements.

Disadvantages of mechanical alloying + sintering:
- Small amount of produced powder;
- Contamination by carbon (graphite), oxygen;
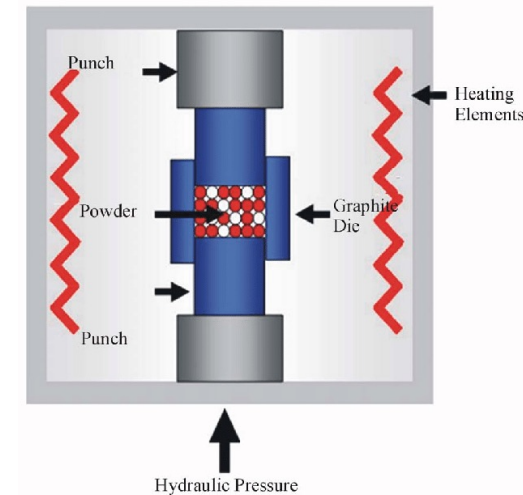- Porosity.
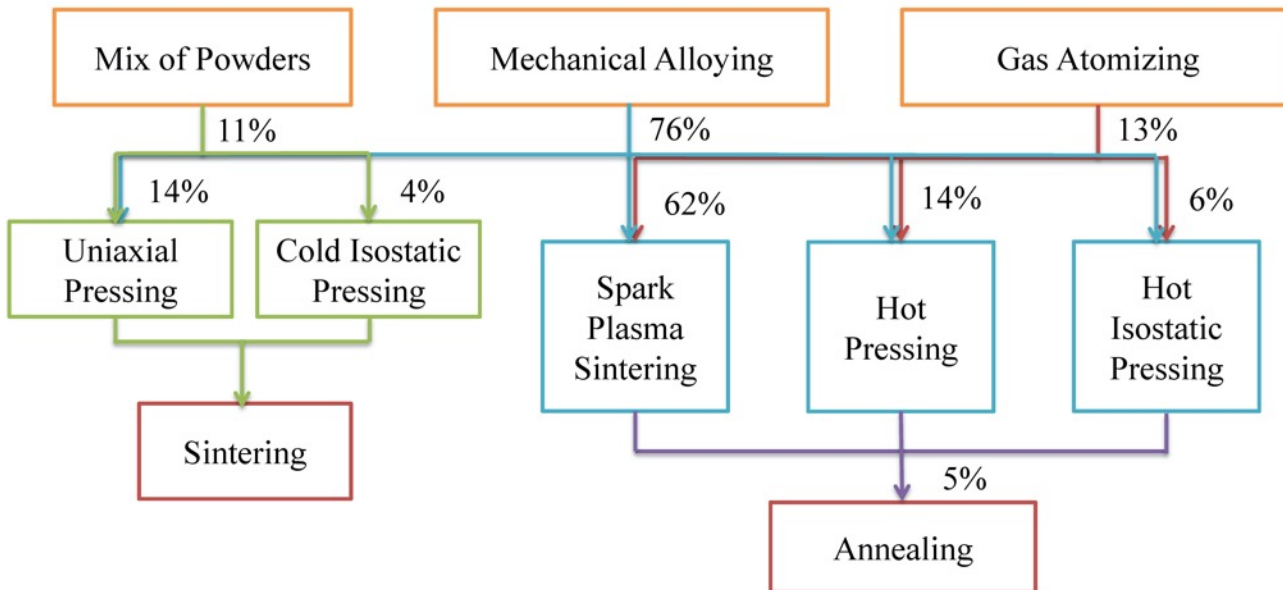
Different powder metallurgy processing routes to obtain HEAs.

J. M. Torralba, P. Alvaredo, A, García-Junceda, Powder Metallurgy 2019, Vol. 62, No. 2, 84-114.
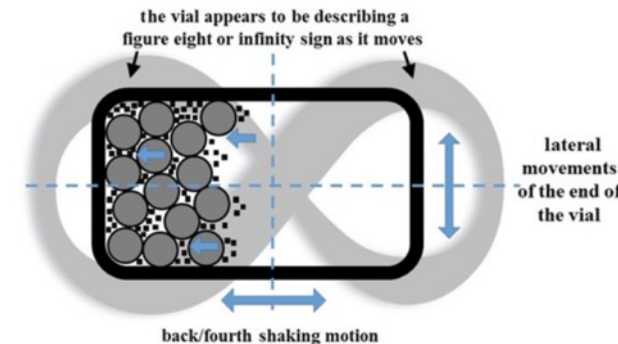
Principle of vibrational mill.

Ashkan Zolriasatein et al., Micro & Nano Letters, 2018,13, 448.

Schematic illustration of hot-press sintering.

S. Moustafa et al., Materials Sciences and Applications, 02(08) (2011) 1127-1133.

2.2.2. FM – solid state – AlCrFeMnMo by powder metallurgy

Studies of new AlCrFeMnMo family with improved mechanical properties.

Why is it complicated to prepare the AlCrFeMnMo by casting?
    Wide range of melting temperatures of elements ➔
    ➔ in case of melting, risk of losing Mn and Al ➔
    ➔ powder metallurgy route (solid-state process)
    preferred for the fabrication of the AlCrFeMnMo alloy.

SPEX vibrational ball mill.

Milling – mechanical alloying conditions:
- Hardened steel balls and vial;
- Ball/powder ratio: 10/1;
- Milling under argon, ~ room temperature;
- 32 x Cycle: 1 h of milling + 0.5 h break;
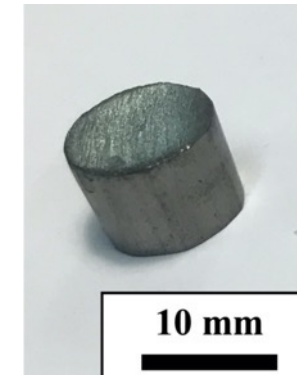- ~ 1.2 g of milled powder.

Sintering conditions (hot-press):
- Graphite matrix (diameter = 10 mm);
- Load: 80 MPa;
- Atmosphere: vacuum or argon;
- Temperatures: 950 and 1100 °C;
- Duration : 1 or 2 h.

*Graphite sintering matrix.*

10 mm

Sintered sample.

Sintering furnace.
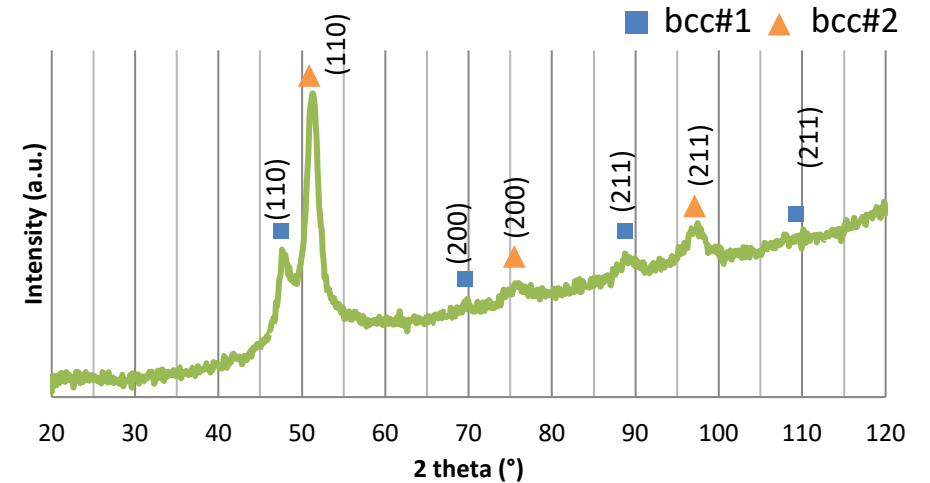
15

2.2.3. FM – solid state – AlCrFeMnMo by powder metallurgy

- Two phase bcc structure after mechanical alloying:
  - bcc#1: a_1 = 3.13 Å;
  - bcc#2: a_2 = 2.93 Å.
- Homogeneous chemical elements distribution at SEM scale.
- Composition:
  - before milling: 22.5% Al, 22.5% Cr, 28% Fe, 20% Mn, 7% Mo
  - after milling: 22% Al, 22% Cr, 30% Fe, 19% Mn, 7% Mo
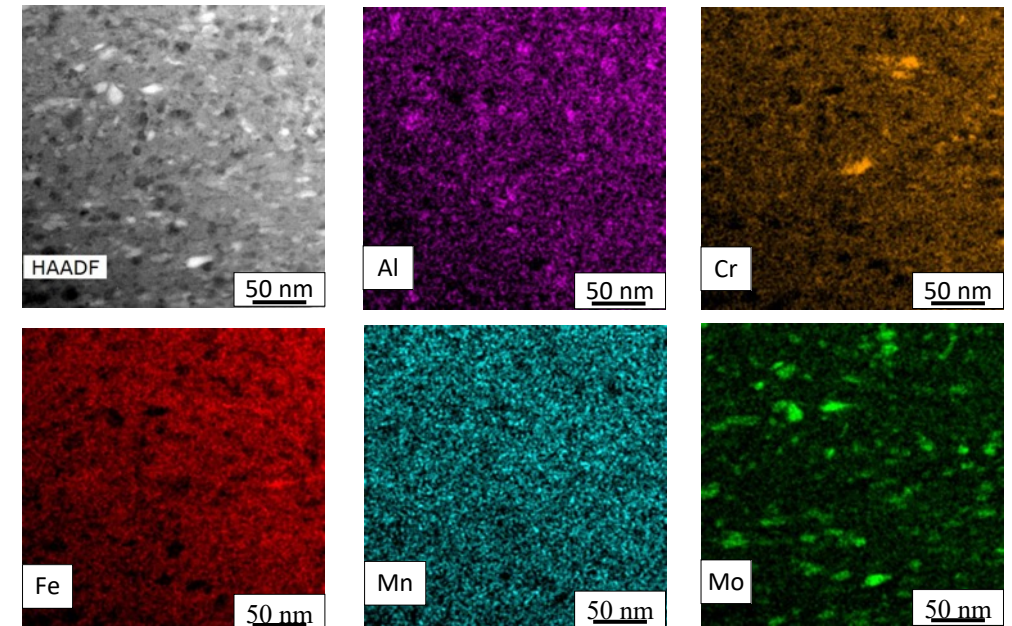- TEM observations: one phase with all elements, the second one rich in molybdenum.

XRD patterns of mechanically alloyed powder.
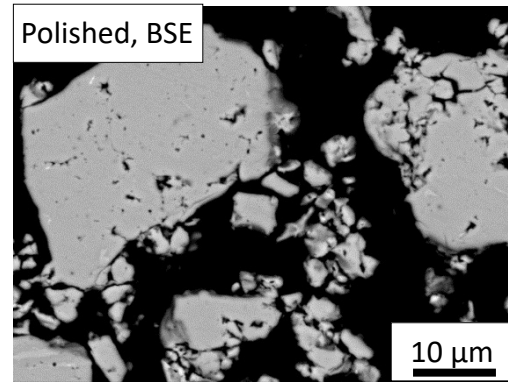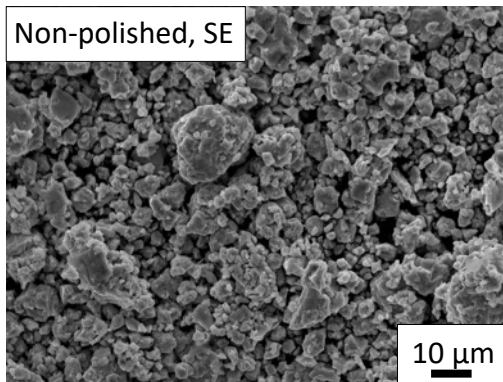
SEM images of milled powders from Al-Cr-Fe-Mn-Mo family.

STEM-EDX map showing chemical elements distribution in mechanically alloyed powder.

16

2.2.4. FM – solid state – AlCrFeMnMo by powder metallurgy

- Bcc#2 - major phase in all sintered samples; bcc#1, present in milled powder, disappears;

- Sintering at 950°C – M_6C the main carbide;

- Sintering at 1100°C – $M_{23}C_6$ the main carbide;

- Small lattice parameters changes due to slightly different chemical composition of formed phases depending on the sintering conditions.

- Black points on SEM-BSE images – porosity ➔ coalescence of the nano-porosity at higher sintering temperature.
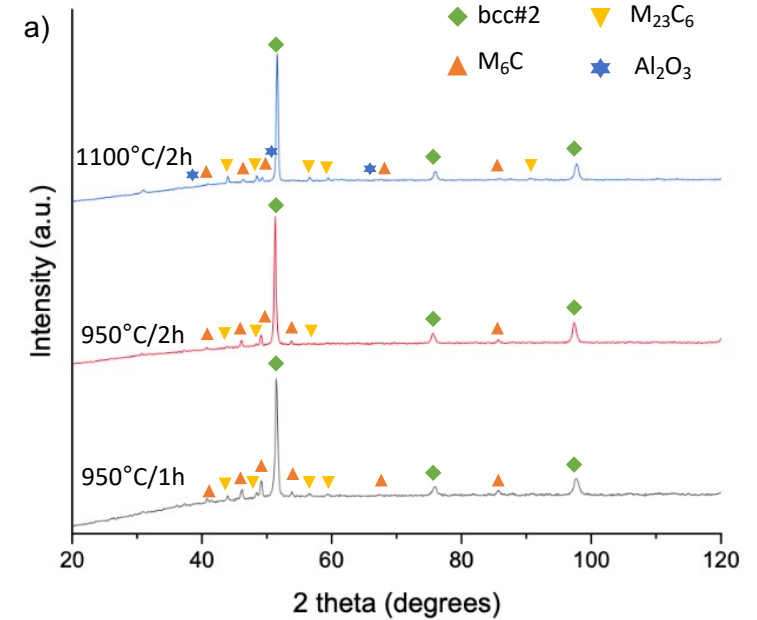
XRD patterns of sintered samples.

| Sample	Lattice parameter [Å]		
	bcc#2	M_6C	$M_{23}C_6$
950 °C/1h	2.92	11.17	10.69
950 °C/2h	2.92	11.18	10.69
1100 °C/2h	2.91	11.16	10.67
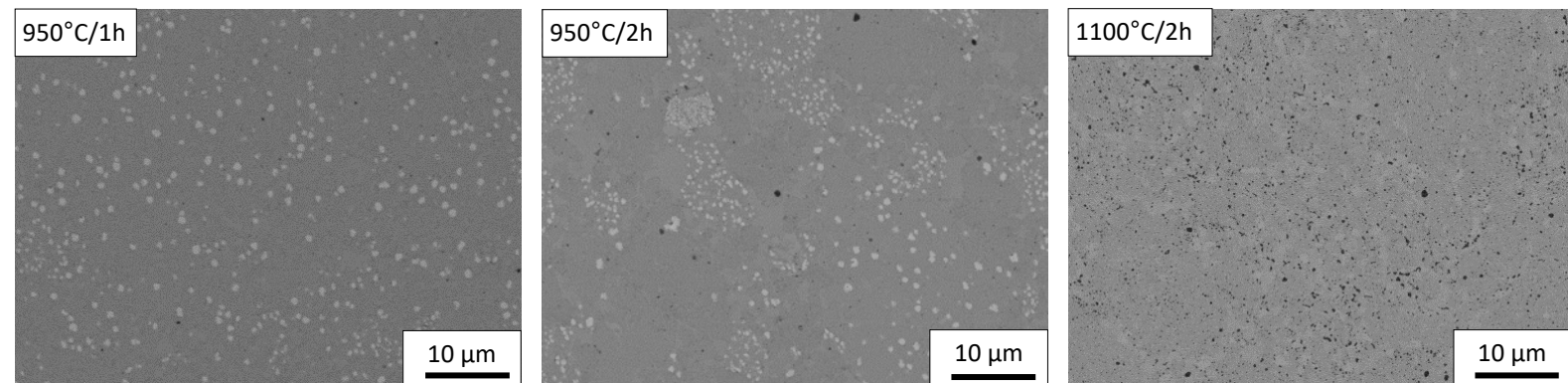
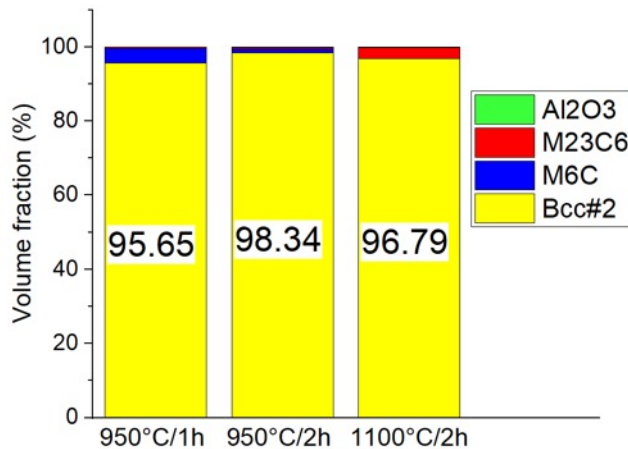*SEM-BSE images of sintered samples.*

2.2.5. FM – solid state – AlCrFeMnMo by powder metallurgy

- Bcc#2 – major phase in all sintered samples.

- Mean grain size of the sintered samples:
  - 950°C/1h: d = 230 nm;
  - 950°C/2h: d = 220 nm;
  - 1100°C/2h: d = 430 nm.

- Abnormal grain growth (grain size > 1 µm, but a large majority of grains < 400 nm in size).
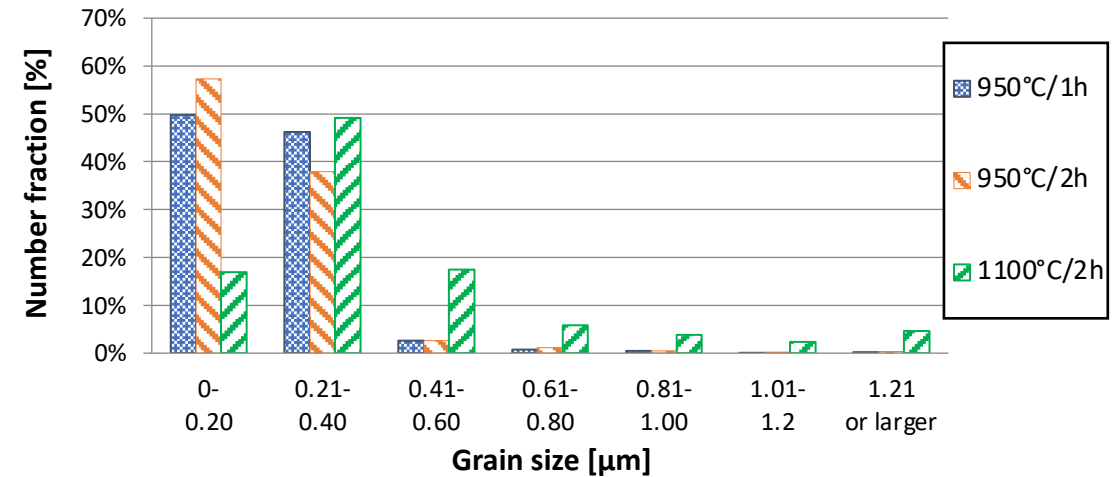
Histograms of grain size of the bcc#2 phase in the sintered samples.

Volume fraction of phases detected by EBSD in the sintered samples.
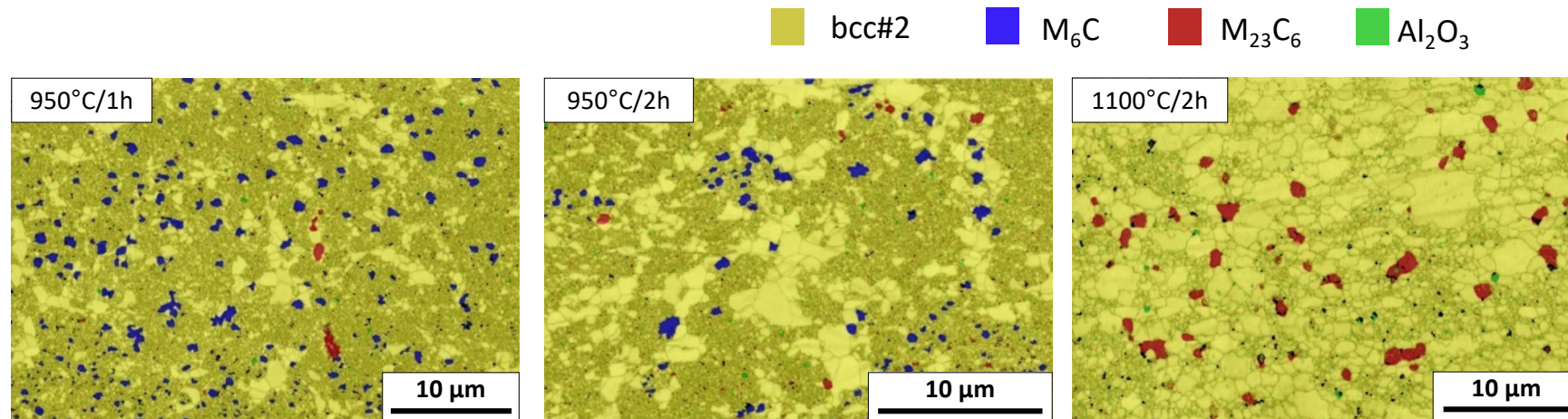
EBSD phase images of sintered samples.

18

2.2.6. FM – solid state – AlCrFeMnMo by powder metallurgy
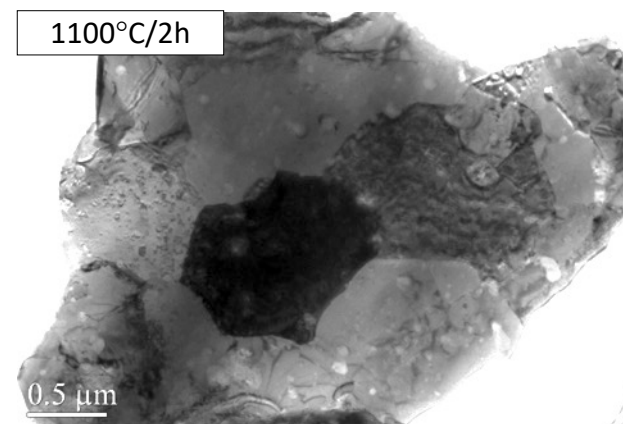
- Observation of the microstructure by TEM to confirm the phases detected by other techniques and analyze the chemical composition of the phases.

- Confirmation of the presence of multielement bcc phase.

- Grain growth with increasing sintering temperature.
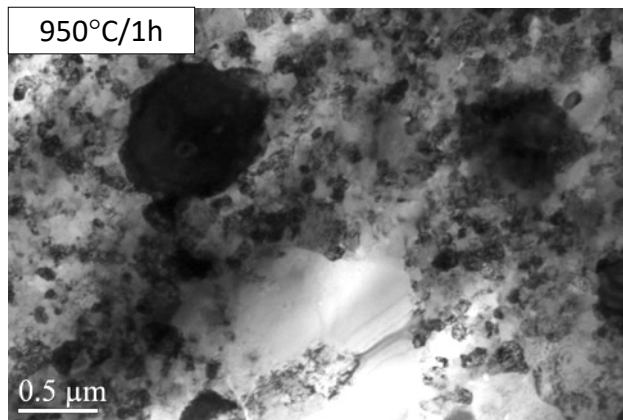
TEM-BF images of samples sintered at 950°C/1h and 1100°C/2h
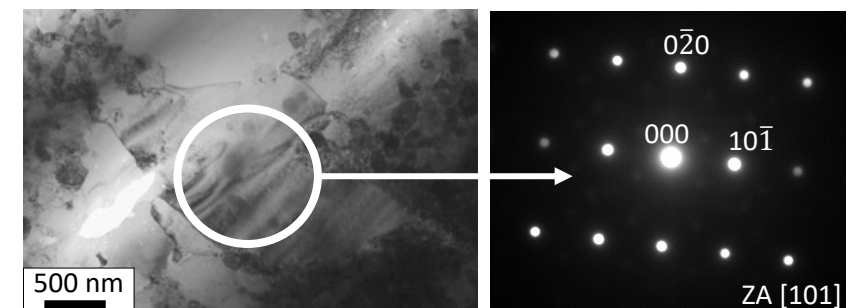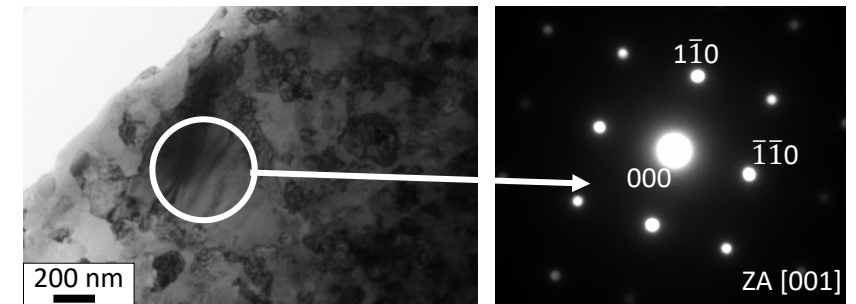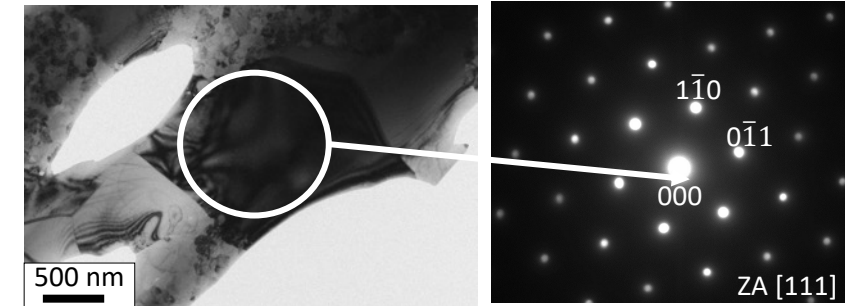
TEM-BF images and SAED patterns of the major bcc phase in different zone axis.

2.2.7. FM – solid state – AlCrFeMnMo by powder metallurgy

- Confirmation of the presence of the phases, related to the contamination, detected by other techniques.

- Presence of two types of carbides:
  - Multielement M_6C carbide – rich in Mo – found mainly in the samples sintered at 950°C;
  - Multielement $M_{23}C_6$ carbide – rich in Cr – found mainly in the sample sintered at 1100°C.

- Grains of alumina (mostly visible in the sample sintered at 1100°C/2h).
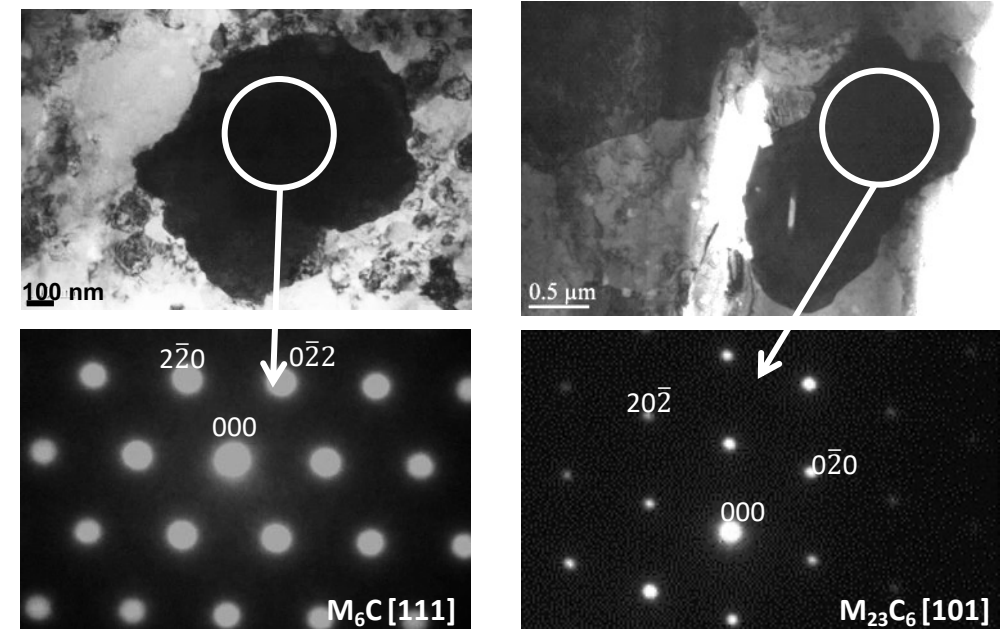
TEM-BF images and SAED patterns of M_6C and $M_{23}C_6$ carbides.

TEM-BF images of Al_2O_3 grains.

Phase	Concentration [at. %]				
	Al	Cr	Fe	Mn	Mo
overall	18.8	22.4	31.5	19.8	7.5
bcc#2	19.0	21.4	33.7	19.2	6.7
M_6C	15.1	13.1	18.7	9.3	43.8
$M_{23}C_6$	3.2	62.5	11.1	13.6	9.6

2.2.8. FM – solid state – AlCrFeMnMo by powder metallurgy

Hardness measurements

- Very high hardness of sintered samples.
- Decrease in hardness for the higher sintering temperature (grain growth).
- Small circumferential cracks (micro-indentation) – no radial cracks.

Compression test

- 20 – 500°C: brittle behavior (small grain size, carbides and oxides, no optimal cohesion between the grains).
- 600 - 800°C: plastic deformation: decrease in yield strength with increasing testing temperature; ductility increases dramatically with increasing testing temperature.
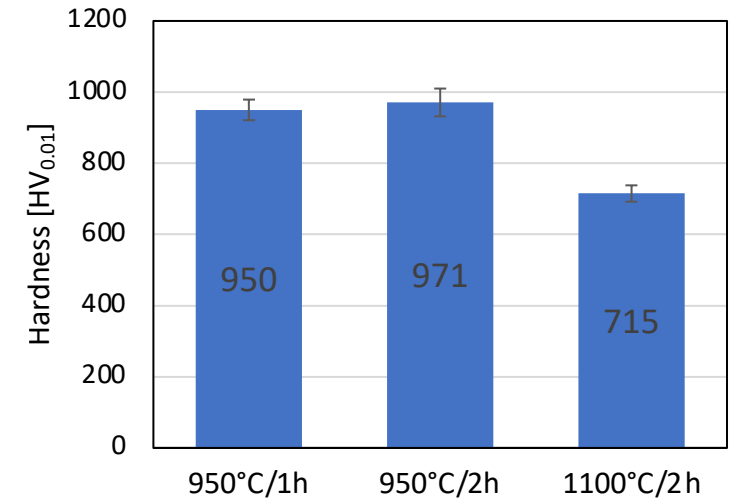
Hardness of the sintered samples measured under a load of 1N.
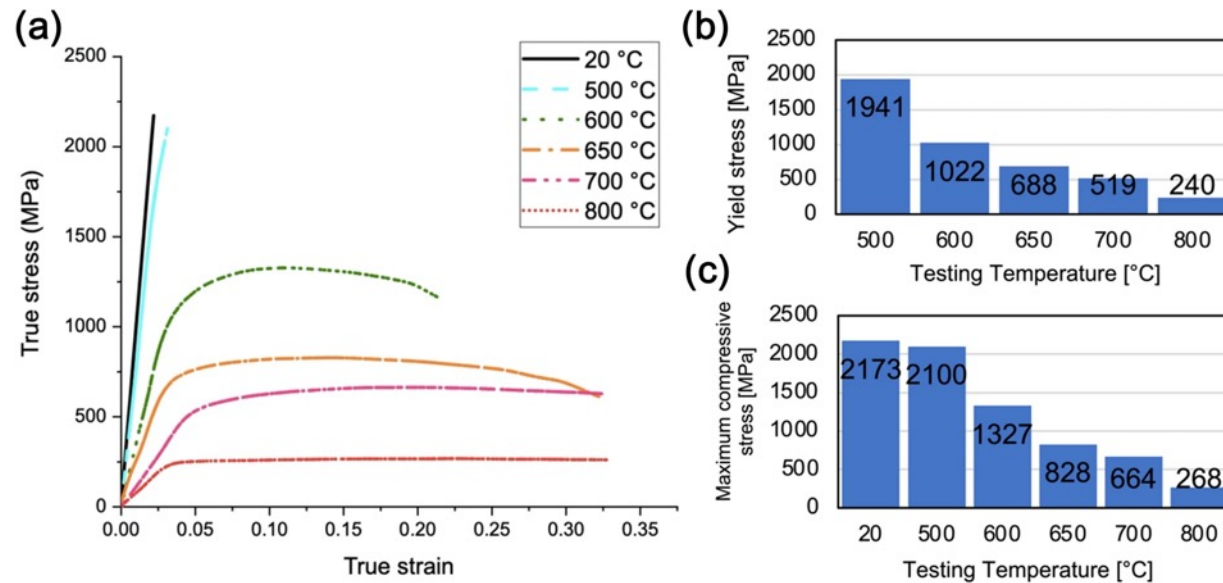
Compression results acquired at strain rate of 10^{-3} s^{-1} at different temperatures of the sample sintered at 950°C/2h.
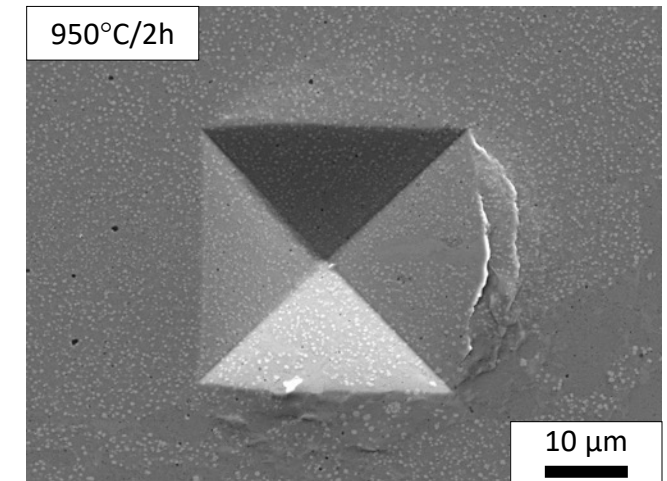
SEM-SE image of indentation site.

2.2.9. FM – solid state – AlCrFeMnMo by powder metallurgy

Conclusions

- HEA from the Al-Cr-Fe-Mn-Mo family successfully prepared by powder metallurgy.

- Mechanical alloying optimized to promote chemical homogeneity of particles (two bcc phases).

- Multielement bcc phase (a ~2.92 Å) major in all sintered optimized samples.

- Small fraction of carbides and alumina due to the contamination during mechanical alloying and sintering.

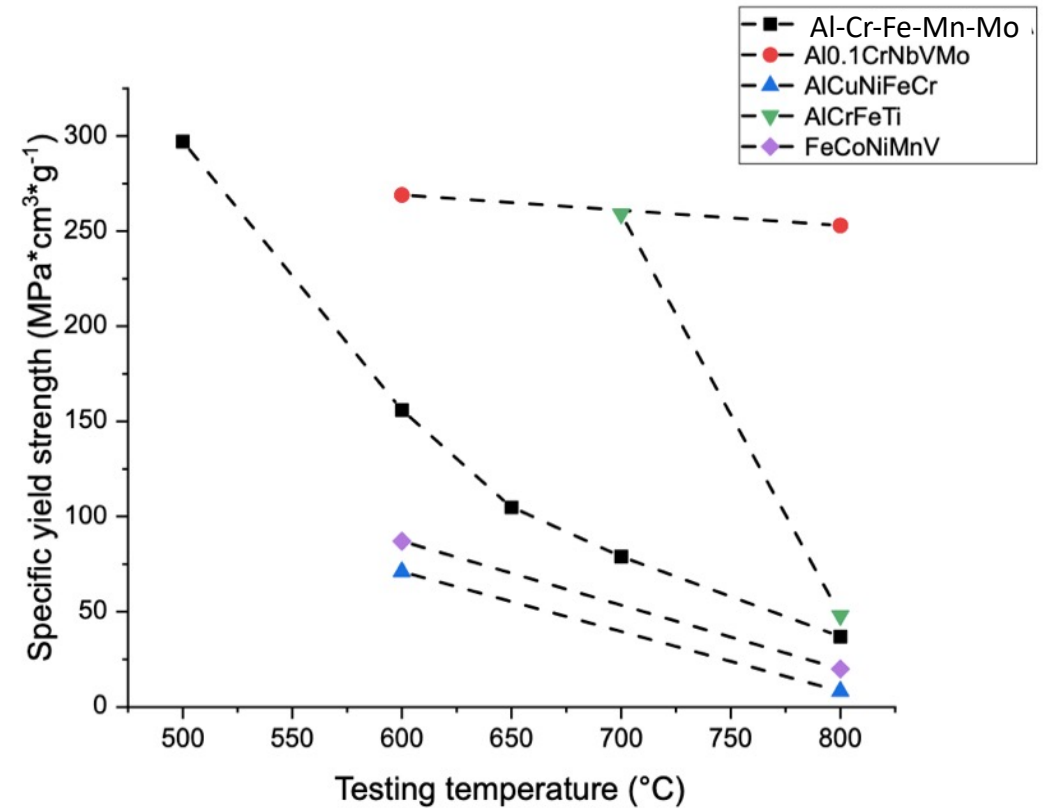- Very fine grains after sintering: 200 nm (950 °C) and 400 nm (1100 °C).

- Very high hardness of sintered samples up to 950 HV_{1N}.

- Very good compression properties, especially between 600 and 700 °C, at 600 °C: yield strength of 1022 MPa and deformation of 21.8%.

Specific yield strength of the Al-Cr-Fe-Mn-Mo alloy compared to other HEAs produced by powder metallurgy $Al_{0.1}CrNbVMo*$, AlCuNiFeCr**, AlCrFeTi***, FeCoNiMnV****.
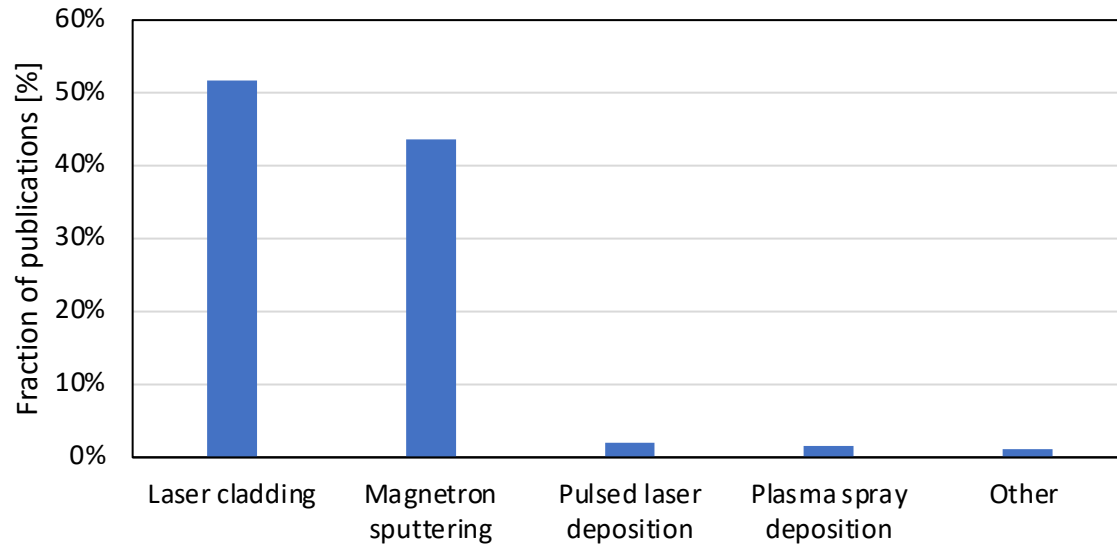
*B. Kang et al., J. Alloys Compd. 767 (2018) 1012–1021.
**A.I. Yurkova et al., J. Alloys Compd. 786 (2019) 139–148.
***D. Shaysultanov et al., Mater. Sci. Eng. A. 795 (2020) 140018.
****F. Alijani et al., Mater. Chem. Phys. 256 (2020) 123675.

2.3.1. FM – coating deposition

Distribution of works published depending on deposition method of HEA coatings.

V. E. Gromov, S. V. Konovalov, Yu. F. Ivanov, K. A. Osintsev, Structure and Properties of High-Entropy Alloys, Springer 2021.

Magnetron Sputtering

- Physical vapor deposition (PVD) method ➔ thin films.
- Knocking out of target materials' atoms by bombardment with incident species (e.g., Ar^+).
- Coating elements could also be introduced via a gas phase ➔ reactive magnetron sputtering.
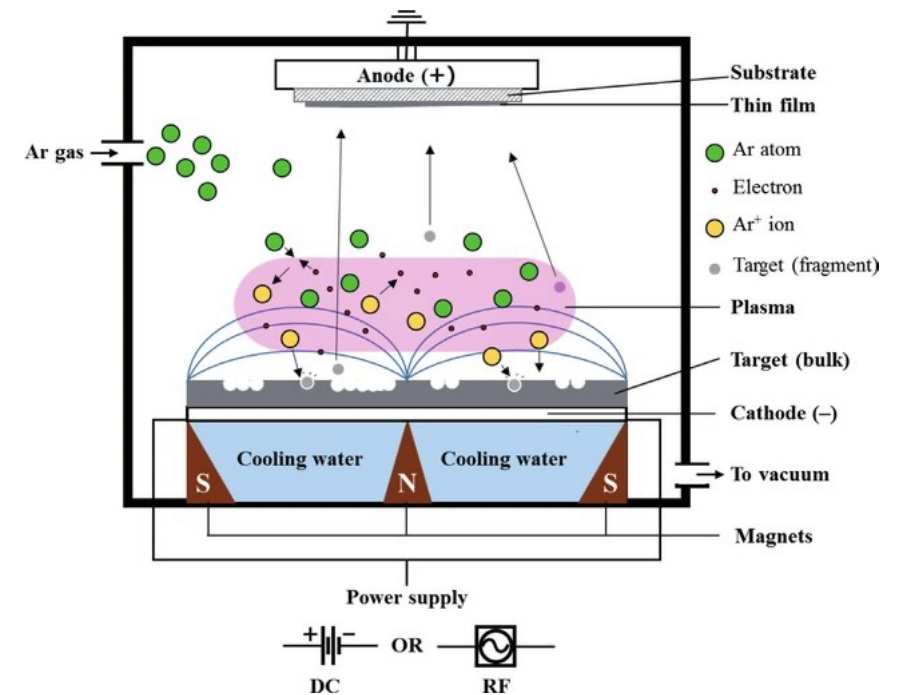
Schema showing principle of magnetron sputtering.

P.N. Hishimone, H. Nagai, M. Sato, Methods of Fabricating Thin Films for Energy Materials and Devices: Lithium-ion Batteries - Thin Film for Energy Materials and Devices, Intechopen 2020.
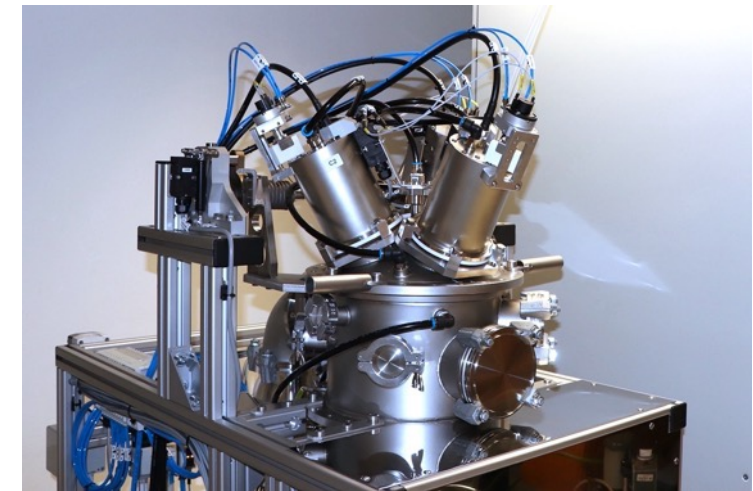
HVM Flexilab - thin film deposition system.

2.3.2. FM – plasma deposition – CrHfMoTaW thin films

HEA concept extended beyond metallic materials to **high entropy ceramics (HECs).**

Especially interesting – deposition of **high entropy nitrides (HENs)** thin films.
- (AlCrTaTiZr)N - the first prepared HEN thin-film*.
- Most commonly fcc single nitride phase.
- High hardness, corrosion, wear, or oxidation resistance.

Our study (deposition of HEAs and HENs form CrHfMoTaW system):
- Elemental segmented targets (2-inch diameter, 3 mm thickness)
- Power supplied:
  - Cathode 1 (Cr): 80 W;
  - Cathode 2 (Hf+Mo): 150 W;
  - Cathode 3 (Ta+W): 150 W.
- Argon flow: 80 sccm + Nitrogen flow: 0-20 sccm ➔ 1.20-1.40 Pa.
- Base pressure: $2 \cdot 10^{-4}$ Pa.
- Deposition time: 30 minutes.
- Rotation of the substrate holder: 5 rpm.
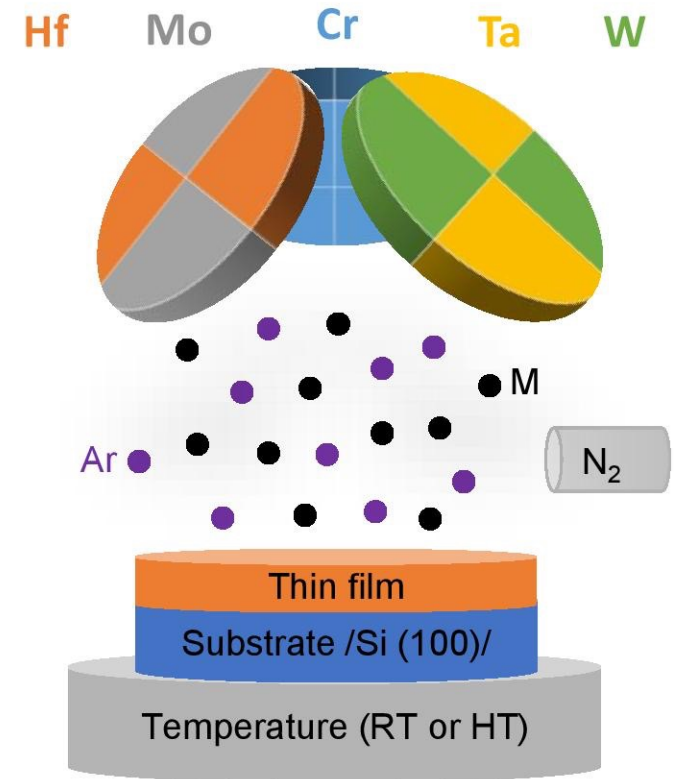
Schema showing magnetron sputtering process in this study.

For more information about deposition of CrHfMoTaW thin films, please refer to our conference proceedings: T. Stasiak, P. Soucek, V. Bursikova, P. Vasina, *Magnetron Sputtering Deposition of High Entropy Nitrides from Cr-Hf-Mo-Ta-W System*, Proceedings NANOCON 2021 conference.

*Chia Han Lai et al., Surf. Coat. Technol. 201, no. 6 (2006): 3275–3280.

2.3.3. FM – plasma deposition – CrHfMoTaW thin films

- Increase of N content with the increasing N_2 flow up to 45.9 at. %.

sccm = standard cubic centimeters per minute

- Structure of the coatings:
    - 0 sccm N_2: metallic bcc phases.
    - 5 sccm N_2: amorphous structure (RT)
    - 10-20 sccm N_2: multielement fcc nitride.
- Increase of lattice parameter with increasing N_2 flow.
- Decrease of crystallite size with increasing N_2 flow.

Composition of coatings vs. nitrogen flow
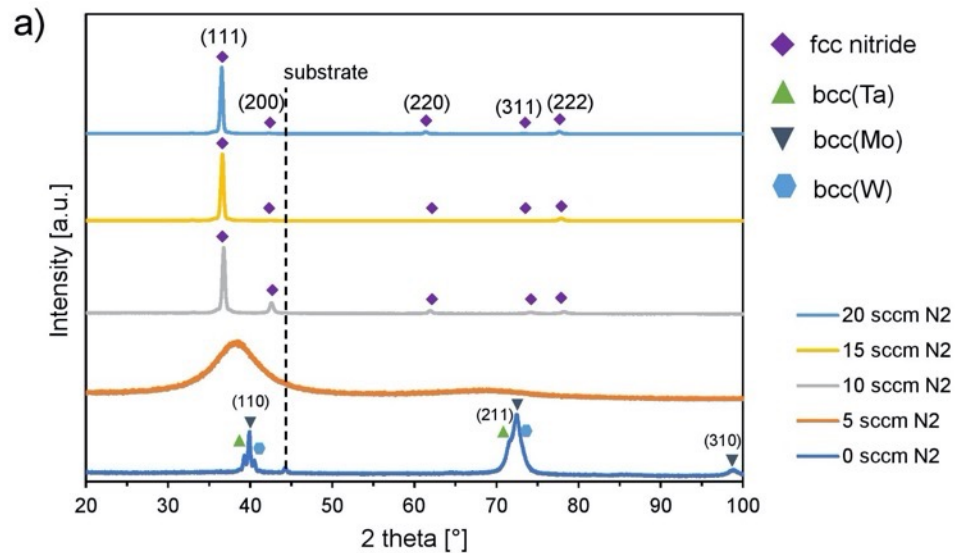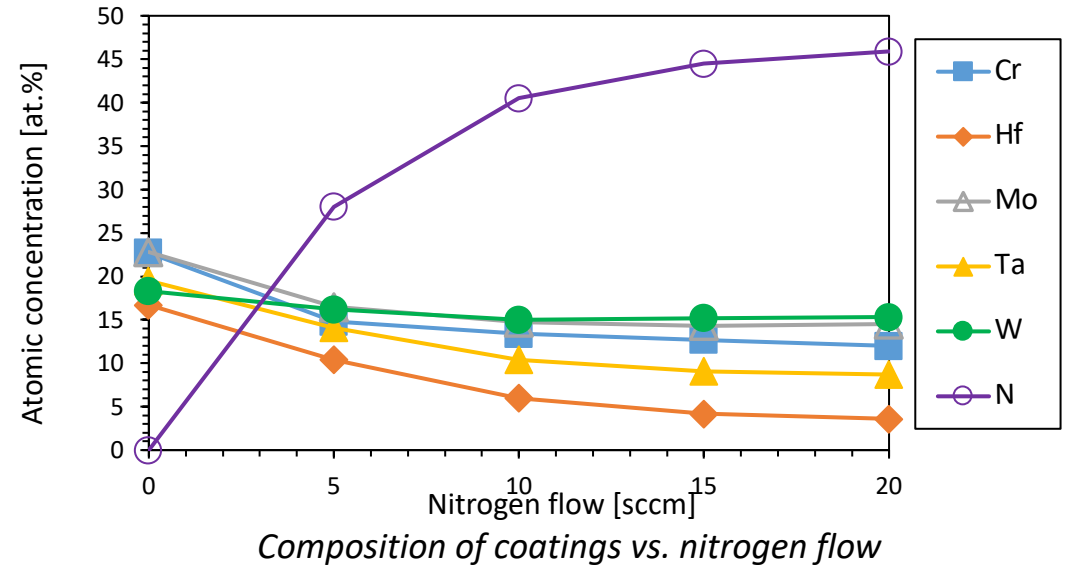
X-ray diffraction patterns of deposited coatings

Crystallite size and lattice parameter vs. nitrogen flow
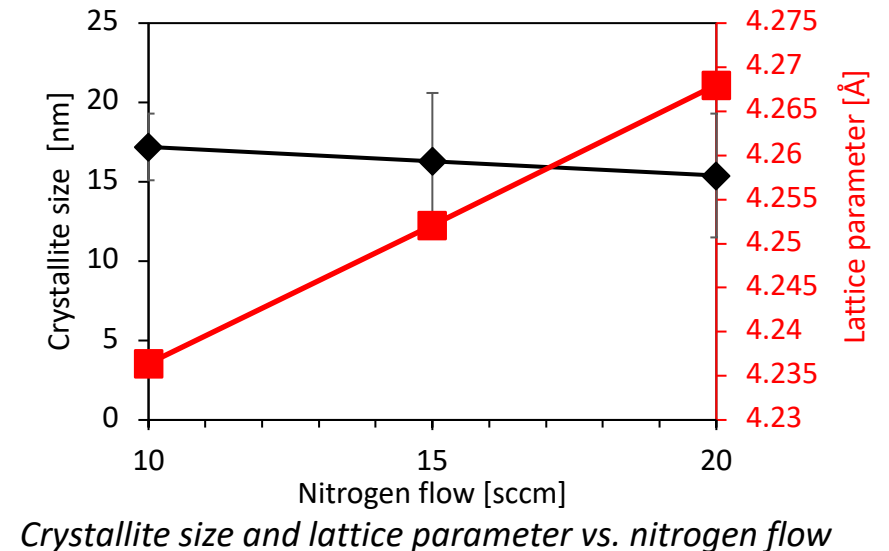
2.3.4. FM – plasma deposition – CrHfMoTaW thin films

- Decrease of deposition rate with increasing N_2 flow ➔ especially between 0 sccm N_2 and 10 sccm N_2 ➔ the effect of poising of targets.
- Similar deposition rate of multielement fcc nitride coatings.

- Metallic coating ➔ columnar microstructure.
- Coating deposited at 5 sccm N_2 ➔ Very dense amorphous structure.
- Coating deposited at (10-20 sccm N_2) ➔ columnar microstructure of fcc nitride coatings.
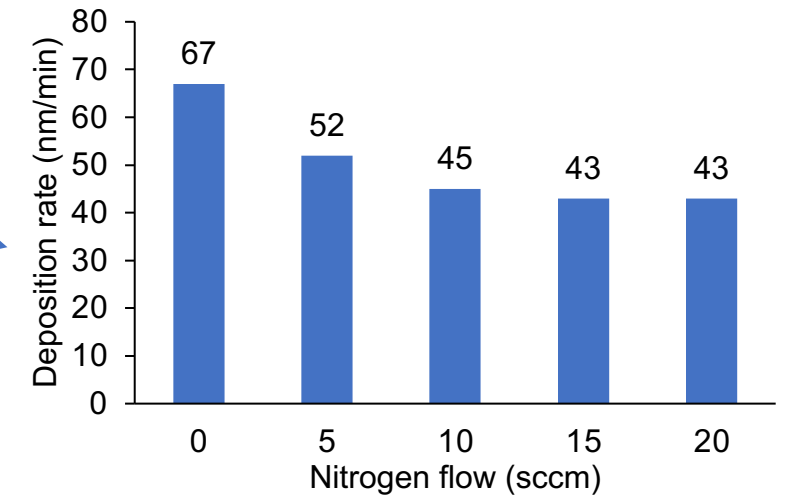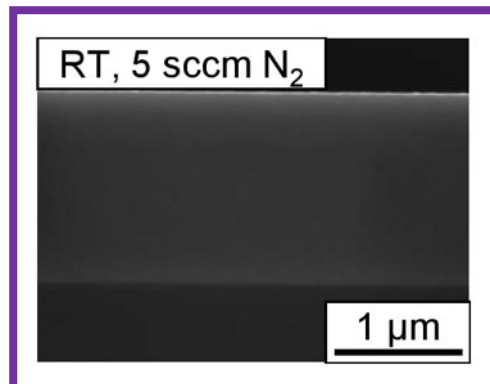

Deposition rate of the coatings deposited under different nitrogen flow.
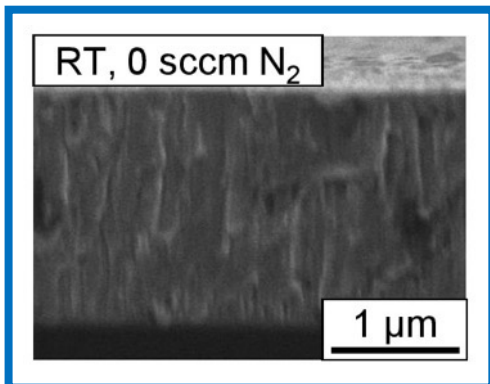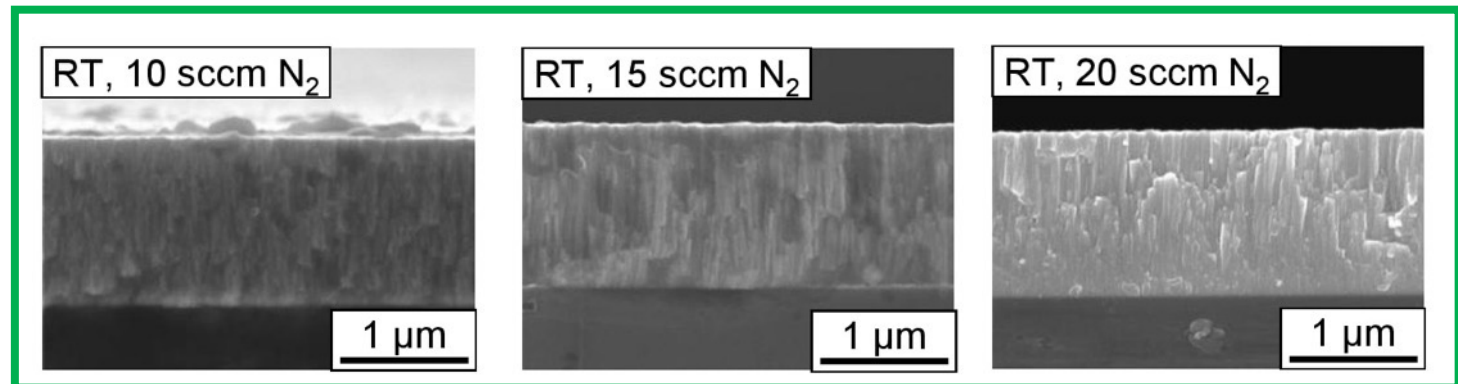
Metallic phases   Amorphous   Fcc multielement nitride

SEM-SE images of the cross-sections of deposited coatings.

2.3.5. FM – plasma deposition – CrHfMoTaW thin films

- High hardness and effective Young's modulus of metallic coatings.

- Very high hardness and effective Young's modulus of amorphous coating ➔ very dense microstructure.

- Hardness and effective Young's modulus of fcc nitride coatings ➔ decrease of hardness and effective Young's modulus with increasing N_2 flow.
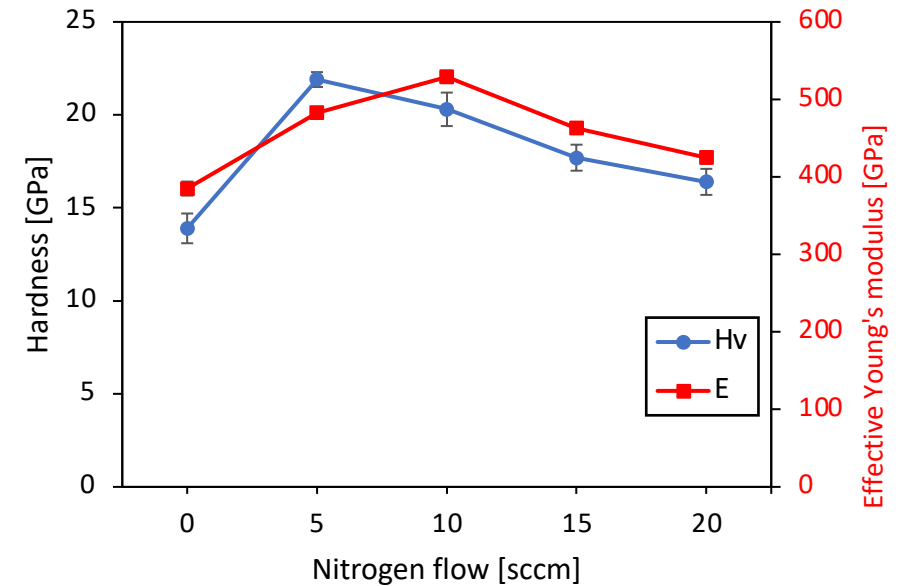
*Hardness and Young's modulus of deposited coatings vs. nitrogen flow.*

Conclusions

- Successful deposition of novel high entropy alloys and nitrides from the **Cr-Hf-Mo-Ta-W** family at room temperature.

- Preparation and investigation of coatings with **metallic bcc** structures (no nitrogen), **amorphous** structure (low flow of N_2), and **multielement fcc nitrides** (higher N_2 flow) with **nanometric grains**.

- Increase of lattice parameter and decrease crystallite size of fcc nitride with increasing N_2 flow.

- High deposition rate of coatings between **67 nm/min and 43 nm/min**.

- High hardness (up to **21.9 GPa**) and effective Young's modulus (up to **529 GPa**) of deposited coatings.

3. Conclusions and future prospects

- High entropy alloys are under the focus of the scientific community due to almost infinite possible new compositions and many promising properties.

- For 13 most commonly used elements, there are 7099 possibilities to develop new equiatomic HEA ➜ development of new screening techniques and simulation methods.

- HEAs reveal a wide range of promising properties, depending on the chemical composition, structure, fabrication technique…

- HEAs are prepared by different types of techniques to produce bulk materials or coatings, e.g.,

  - Casting;

  - Powder metallurgy;

  - Additive manufacturing;

  - Deposition techniques (PVD).

- The potential of further development is almost unfinished.

3.1. Future prospects – High Entropy Shape Memory Alloys (HESMA)

- HESMA – new group of materials introduced in 2015 by Firstov et al.* to extend the range of applications of shape-memory materials.

- Shape memory effect – the ability of deformed material to return to its pre-deformed shape upon thermal treatment.
- The most studied traditional shape memory alloy – NiTi.

- Advantages of HESMAs over traditional shape memory alloys:
  - Higher transformation temperatures,
  - Smaller decrease of transformation temperatures with thermal cycling.
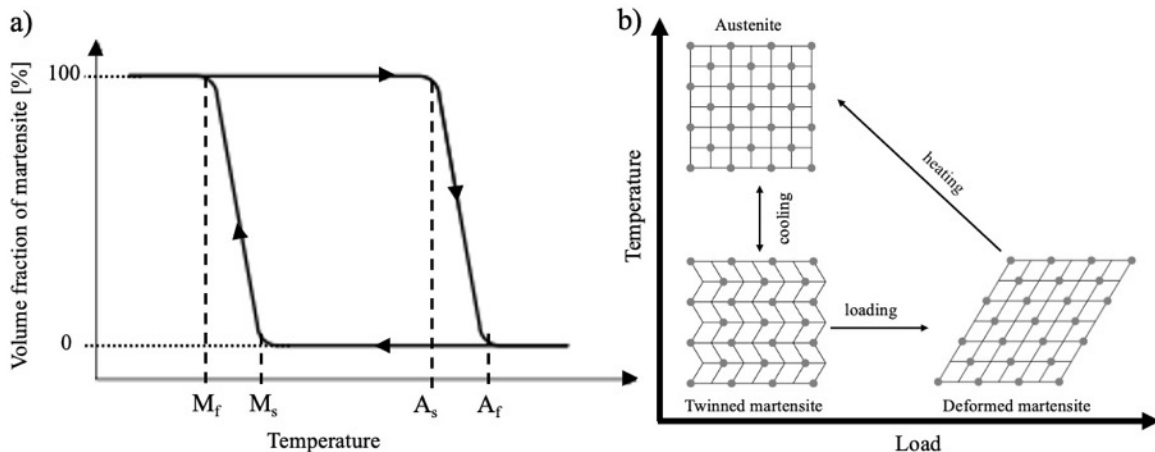
Schematic diagrams of a) temperature–transformation curve of a heating-cooling cycle of an SMA, b) events in a material revealing shape memory effect.
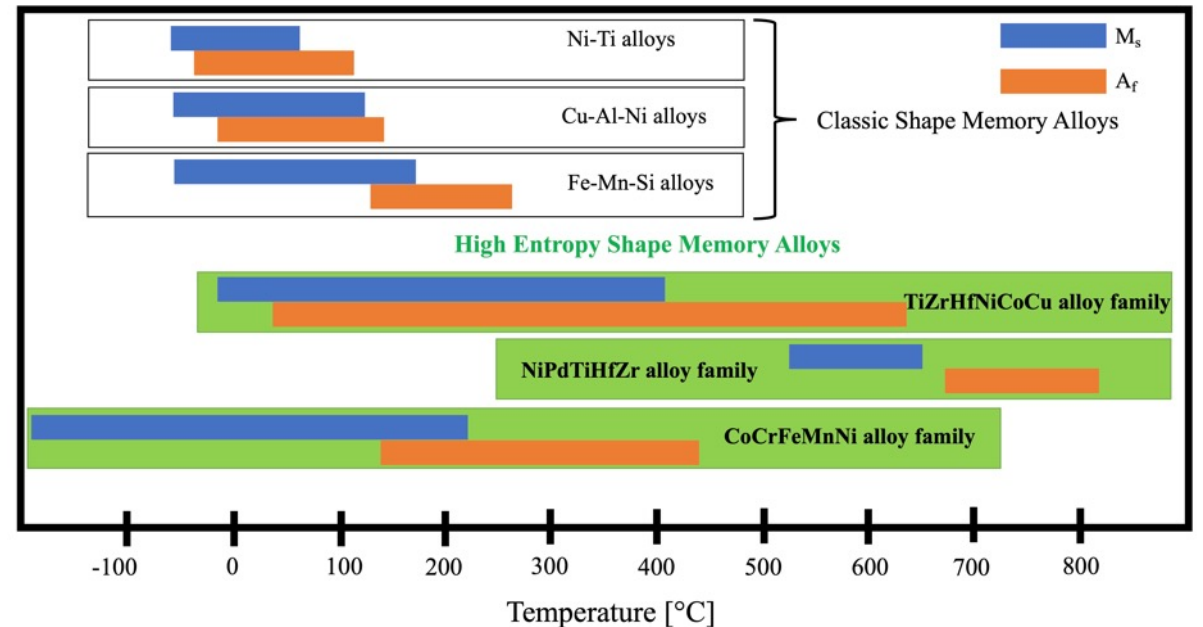
Ranges of transformation temperatures (M_s and A_f) of commonly studied classic SMAs and new HESMAs prepared by the liquid route.

*G.S. Firstov, T.A. Kosorukova, Y.N. Koval, V. V. Odnosum, Mater. Today Proc. 2015, S499–S503.

Thank you for your attention!

Tomasz Stasiak

Masaryk University, Brno, Czech Republic

E-mail: t.stasiak@yahoo.pl